

Review

Spatial omics at the forefront: emerging technologies, analytical innovations, and clinical applications

Yunhe Liu,¹ Yibo Dai,^{1,2} and Linghua Wang^{1,2,3,4,*}¹Department of Genomic Medicine, The University of Texas MD Anderson Cancer Center, Houston, TX 77030, USA²The University of Texas MD Anderson Cancer Center UTHealth Houston Graduate School of Biomedical Sciences, Houston, TX 77030, USA³The James P. Allison Institute, The University of Texas MD Anderson Cancer Center, Houston, TX 77030, USA⁴Institute for Data Science in Oncology, The University of Texas MD Anderson Cancer Center, Houston, TX 77030, USA*Correspondence: Iwang22@mdanderson.org<https://doi.org/10.1016/j.ccr.2025.12.009>

SUMMARY

Spatial omics transforms our understanding of cancer by revealing how tumor cells and the microenvironment are organized, interact, and evolve within tissues. Here, we synthesize advances in spatial technologies that map tumor ecosystems with unprecedented fidelity. We highlighted analytical breakthroughs—including multimodal integration and emerging spatial foundation models—that resolve functional niches and spatial communities, converting spatial patterns into mechanistic insights. We summarize how spatially organized features, from immune hubs to microbiota and neural interfaces, shape tumor evolution and clinical outcomes. We then outline how spatial approaches illuminate precancer biology, metastatic adaptation, and therapy response. Bridging discovery and translation, we provide a practical roadmap for incorporating spatial readouts into clinically oriented study design. We conclude by discussing persistent challenges in standardization and scalability and how high-plex spatial discoveries may be distilled into scalable, AI-enabled, clinically deployable assays, positioning spatial omics as a cornerstone of next-generation predictive and precision oncology.

INTRODUCTION

Cancer is a highly heterogeneous disease characterized by intricate interactions between tumor cells and the tumor microenvironment (TME). Over the past decade, single-cell omics have provided critical insights into the genetic, epigenetic, and transcriptional programs underlying tumor biology and immunobiology.^{1,2} However, these approaches often lack the spatial context essential for resolving tissue architecture, cell-cell interactions, and functional niches that orchestrate immune responses, tumor evolution, and therapeutic outcomes.

The emergence of spatial omics technologies, including spatial transcriptomics, spatial proteomics, and highly multiplexed molecular imaging, has marked a paradigm shift in cancer research.^{3–7} These platforms enable high-resolution *in situ* characterization of transcriptomic and proteomic landscapes, intercellular communication, metabolite gradients, and even genomic alterations and tumor-associated microbiomes, offering unprecedented opportunities to dissect the coordinated organization and dynamic interactions of cells within intact tissues.^{8–10} Coupled with analytical innovations, particularly machine learning-based multimodal data integration, and advances in computational pathology, these approaches are redefining our ability to decode tumor ecosystems, uncover novel biomarkers and therapeutic targets, and elucidate disease mechanisms *in situ*.

Despite these advances, critical challenges remain. Trade-offs in spatial resolution, feature coverage, and scalability, alongside analytical and standardization hurdles, have limited broader translational adoption. Overcoming these barriers is essential to fully realize the translational potential of spatial omics in precision oncology, a theme explored in depth in later sections.

The field is now entering a new phase focused on improving accessibility, advancing integrative computational frameworks, and expanding clinically oriented applications. Here, we review recent progress in spatial omics, highlighting emerging technologies, analytical innovations, and their applications in decoding TME complexity. We further outline key innovations and strategic directions defining the next era of spatial cancer research.

RECENT ADVANCES IN SPATIAL OMICS TECHNOLOGIES

With the spatial revolution sweeping across the field, an increasing number of proof-of-concept spatial omics technologies have rapidly emerged.^{11–14} Commercialization has been largely driven by practical workflows, standardized data structures, companion analysis tools, and improved cost-effectiveness. Meanwhile, growing demand for larger panels, higher accuracy, enhanced resolution, and multi-modal capabilities¹⁵ has accelerated the transition of these technologies into accessible platforms. In this section, we review widely adopted commercial platforms (Figure 1), encompassing spatial



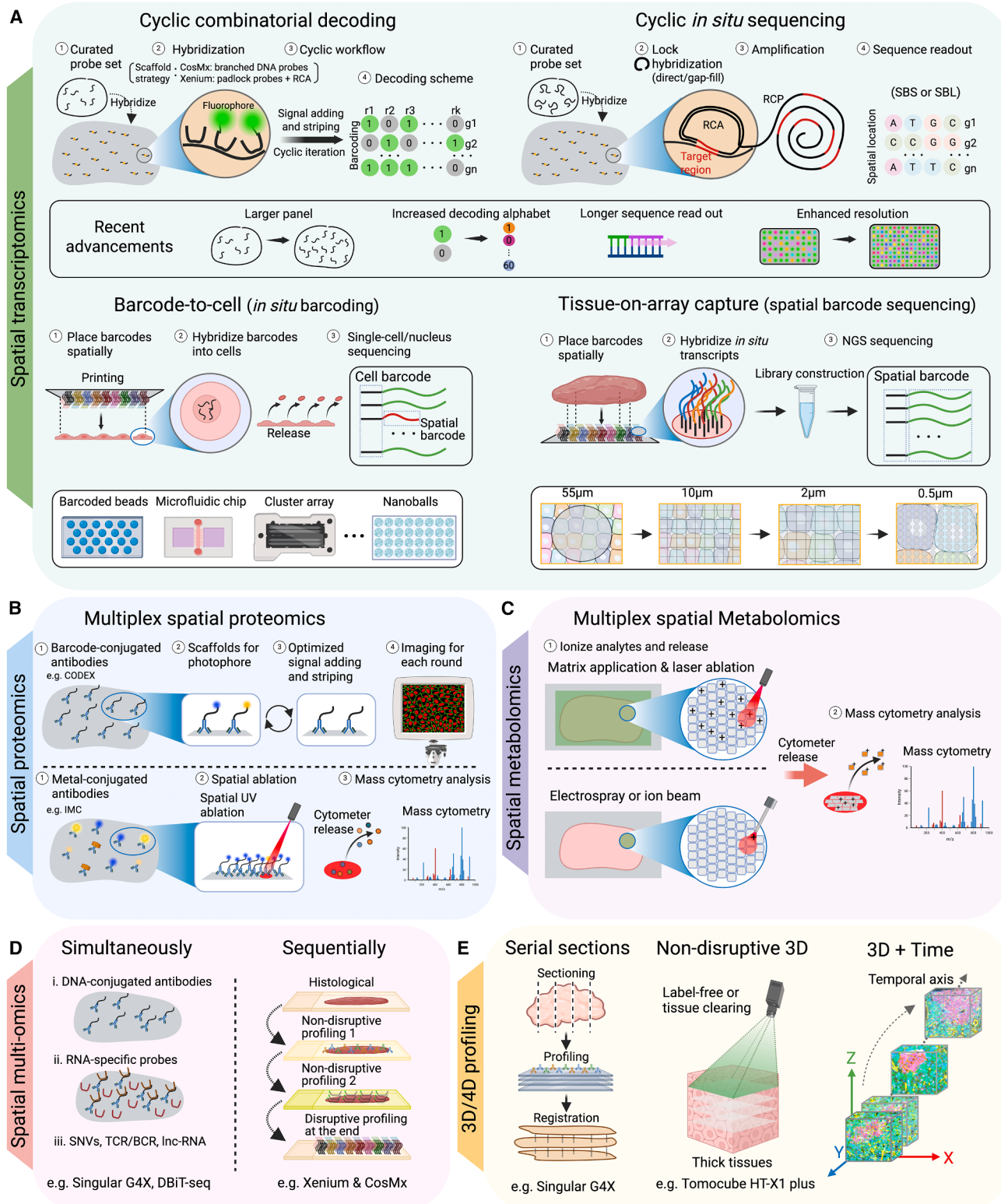


Figure 1. Overview of spatial omics technologies

(A) Spatial transcriptomics. *In situ* (imaging)-based approaches (top) are categorized into cyclic decoding (top left) and cyclic *in situ* sequencing (top right). Spatial barcoding (sequencing)-based approaches (bottom) are subdivided into barcode-to-cell delivery, followed by single-cell sequencing (bottom left) and spatially barcoded capture arrays (tissue-on-array NGS) (bottom right).

(legend continued on next page)

transcriptomic, proteomic, and metabolomic modalities; we highlight their distinctive capabilities, applicability, and tissue compatibility, and discuss ongoing challenges and future directions for advancing the field.

Recently available spatial omics platforms

Spatial transcriptomics

Multiple strategies have emerged for hybridizing or capturing transcripts *in situ* while preserving spatial information. These strategies, reviewed elsewhere,^{15–20} are commonly categorized into imaging-based and sequencing-based approaches. Here, we focus on advanced commercialized technologies (Table 1), further clarifying their subcategory differences within the two major types. For imaging-based methods, we distinguish between cyclic combinatorial decoding and cyclic *in situ* sequencing, which primarily differ in how target identity is readout (fluorescent codes vs. base calls). For sequencing-based methods, we distinguish between tissue-on-array capture (spatial barcode sequencing) and barcode-to-cell (*in-tissue* barcoding), which differ in the mechanism by which spatial coordinates are linked to transcripts^{20,21} (Figure 1).

Cyclic decoding. The basic principle of *in situ*-based technologies (Figure 1A top) is to directly observe transcripts via targeted fluorescence. Fluorescence *In Situ* Hybridization (FISH) and its variants^{22–25} combine RNA probe-based targeting with high-resolution microscopy for single-transcript detection. While iterative hybridization cycles allow multiplexing, panel size remains limited due to practical constraints on the number of iterations. Higher multiplexity is therefore achieved via cyclic combinatorial decoding or cyclic *in situ* sequencing. Cyclic decoding approaches hybridize probe sets targeting hundreds to thousands of genes and decode information via iterative cycles. Technologies differ in probe design, probe architecture (e.g., scaffold-based signal amplification in CosMx,²⁶ or *in situ* rolling-circle amplification (RCA) in Xenium²⁷), fluorophore amplification/removal between cycles, and encoding schemes (e.g., MERFISH-style Hamming codes²⁸). Leading commercial platforms include Xenium *In Situ* (10x Genomics)²⁷ and CosMx (Bruker),²⁶ with their latest platforms and pre-designed panels—Xenium Prime 5K, CosMx 6K, and CosMx whole transcriptome (WTX) panels—detecting up to 5,000, 6,000, and 18,000 genes, respectively.^{11,20} CosMx enables near-whole-transcriptome profiling and supports custom add-on RNA panels of up to 50 genes or standalone panels of up to 300 genes. Xenium also provides extensive flexibility, allowing stand-alone custom panels of up to 480 genes and add-on panels of up to 100 targets, including probes for microbial sequences, single nucleotide variants, isoforms, and T and B cell receptor (TCR/BCR) regions. Both platforms provide dedicated data visualization and analysis tools: Xenium Explorer for Xenium and AtoMx for CosMx.

Cyclic *in situ* sequencing. In contrast, cyclic *in situ* sequencing reads out target RNA sequences directly via synthesis (SBS, e.g., FISSEQ²⁹ and Singular G4X) or ligation (SBL, e.g., STARmap³⁰). Targeted implementations typically hybridize padlock probes (with or without gap-fill), followed by RCA to

create clonally amplified “rolonies” for iterative sequencing. In SBL, the readout is defined by ligated interrogation oligos (either gene-specific barcodes or short endogenous sequence in gap-fill designs), whereas SBS can read contiguous endogenous sequence within the amplified cDNA. Commercialized platforms such as Singular Genomics’ G4X Spatial Sequencer directly sequence targeted regions, including highly variable sequences (e.g., TCR/BCR regions), enabling high-resolution *in situ* multi-omics that is both high throughput and cost-effective. A key limitation, however, is the short-read constraint (~100 bases) and the targeted nature of current panels. This limitation arises from the restricted number of iteration cycles and the diffraction-limited resolution of microscopes, which hampers the ability to resolve densely packed transcripts. To address these challenges, alternative high-resolution strategies have emerged; for instance, seqFISH+,³¹ which encodes each barcode base with 60 pseudo-color channels, enables the detection of >10,000 genes in tens of imaging rounds. Similarly, ExSeq³² enhances spatial resolution by ~4x by physically expanding RNA distributions within a swellable hydrogel. While promising, both approaches are constrained by substantial protocol complexity and demanding imaging and analysis requirements, and key practical considerations, such as throughput, target coverage, cost, and FFPE versus frozen compatibility, remain important drivers for further technical advances.

Barcode-to-cell (*in situ* barcoding). This approach (Figure 1A bottom left) deposits barcodes directly onto tissue, either by hybridizing them with intracellular mRNA (e.g., ZipSeq,³³ XYZeq,³⁴ and sci-Space³⁵) or by tagging individual cells or nuclei (e.g., Slide-tag³⁶). When coupled with single-cell (scRNA-seq) or single-nucleus RNA sequencing (snRNA-seq), this approach enables transcriptome profiling at single-cell resolution while preserving spatial context. While earlier methods achieved only regional resolution (typically 50–200 μm), newer technologies such as Slide-tags³⁶ now offer true single-cell precision by utilizing high-density bead arrays, with cell locations inferred from acquired barcodes. Trekker, a commercialized platform, uses UV light to fix spatial barcodes onto nuclei within tissue sections. These strategies face limitations, including variable capture efficiency, potential spatial biases that may leave regions or cell populations underrepresented, and a lack of direct cell morphology and subcellular detail.

Tissue-on-array capture (spatial barcode sequencing). This strategy (Figure 1A bottom right) links *in situ* transcripts to spatial barcodes on a substrate, followed by next-generation sequencing (NGS).²⁰ The key differences among these approaches lie in the type of substrate used to carry spatial barcodes. Examples include DNA-barcoded beads (Slide-seq^{37,38} and HDST³⁹), microfluidic channels (DBiT-seq⁴⁰), clustered arrays (Seq-Scope⁴¹), DNA nanoballs (Stereo-seq⁴²), and polyacrylamide gel (Pixel-seq⁴³). These variations result in spatial resolutions ranging from 55 μm to 500 nm. Prominent commercialized platforms in this category include Visium (55 μm DNA-barcoded spots), Visium HD (2 μm bins), Stereo-seq (DNA nanoballs,

(B) Spatial proteomics overview.

(C) Spatial metabolomics overview.

(D) Emerging spatial multi-omics, including co-detection (left) and sequential detection (right) strategies.

(E) 3D/4D spatial profiling: serial-section reconstruction (left), non-disruptive volumetric 3D imaging (middle), and 4D spatiotemporal profiling (right).

Table 1. Comparison of major commercial high-resolution spatial transcriptomic profiling platforms

Platform	Category	Resolution	Coverage		Tissue compatibility	Throughput/capture area	Run cost
			RNA	Protein			
Xenium 5K (10x Genomics)	Padlock probes + RCA; imaging-based cyclic decoding	Single molecule (subcellular)	5,000 + custom add-ons	~27-plex	FFPE and FF	Imageable area 12 × 24 mm per slide; 2 slides/run	\$\$\$\$
CosMx SMI 6K/WTX (Bruker)	Branched probes; imaging-based cyclic decoding	Single molecule (subcellular)	~6,000 (6K)/~18,000 (WTX)	~68-plex	FFPE and FF	FOV-based imaging (0.6–0.8 mm ² ; ~3M cells/slide; ≤4 slides/run)	\$\$\$\$
MERSCOPE Ultra (Vizgen)	Error-robust barcoded; imaging-based cyclic decoding	Single molecule (subcellular)	~1,000	~6 proteins	FFPE and FF	Imaging area up to ~3 cm ² per slide	\$\$\$\$
G4X (Singular Genomics)	Direct-Seq™ RNA; cyclic <i>in situ</i> sequencing	Single molecule (subcellular)	~300–500	~17-18-plex	FFPE	Multiple sample formats (e.g., 4.5 × 4.5 mm and 10 × 10 mm) per flow cell; parallel processing	\$\$ - \$\$\$
Visium HD (10x Genomics)	2 μm squares (continuous tiling); spatially barcoded capture	2 μm squares (subcellular)	Whole transcriptome (3' capture)	In development	FFPE and FF	Slide with two 6.5 × 6.5 mm capture areas	\$\$\$
Stereo-seq (STOMics)	Patterned DNA nanoball array; spatially barcoded capture	~500 nm center-to-center (subcellular)	Whole transcriptome	100+ with Stereo-CITE	FF and FFPE (V2/OMNI workflows)	Small to ultra-large format up to 13 × 13 cm	\$\$\$ -\$\$\$\$

Note: Table 1 compares major commercial platforms that are either widely adopted or represent the latest and emerging high-resolution technologies; this list is not exhaustive. Specifications, throughput, and cost are vendor- and site-dependent (2025 estimates). Abbreviations: FFPE, formalin-fixed paraffin-embedded; FF, fresh frozen; FxF, fixed frozen.

500 nm), and Illumina's upcoming spatial platform (flow cell chip, ~600 nm). The strategy's strength lies in its ability to capture whole-transcriptome data efficiently, but achieving single-cell resolution remains a major challenge because spatial barcodes are arranged in a predefined pattern that does not match actual cell boundaries and cells are irregularly shaped; as a result, even on "subcellular-resolution" platforms, barcode units rarely correspond precisely to single-cell boundaries.^{44,45}

Spatial proteomics

Compared with spatial transcriptomics, spatial proteomics offers distinct advantages, including robust single-cell resolution with preserved tissue morphology and direct use of canonical protein markers for accurate cell and structure typing (for example, CD31 to label vascular endothelium or PNAd to identify high endothelial venules, where no single transcript equivalently defines the phenotypes). However, challenges remain regarding panel standardization and quantitative calibration. Most commercialized platforms (Figure 1B) currently detect ~20–60 proteins, with only a few capable of exceeding 100-plex. This restricted multiplexity is driven primarily by the availability of highly specific antibodies, potential cross-reactivity in complex panels, and spectral or cycle-number limitations inherent to fluorophore-based detection. Representative platforms include PhenoCycler-Fusion 2.0 system (formerly CODEX⁴⁶; Akoya Biosciences) with its PhenoCode Discovery IO60 Human Protein panel (60-plex). Similar to the CODEX assay scheme, CosMx offers validated protein assays up to 68-plex; Xenium provides

optional in-line protein expression via protein subpanels (~20-plex in simultaneous RNA+protein runs); and Singular Genomics G4X currently supports 17-plex spatial proteomics alongside RNA in a single run. The Imaging Mass Cytometry (IMC)⁴⁷ platform (Standard BioTools) enables a detection of 40-plus markers using metal-conjugated antibodies with laser ablation and mass spectrometry. The COMET platform (Lunaphore) enables rapid, flexible up to ~40-plex mIF panels using standard label-free antibodies.

These platforms differ in their detection strategies. For example, PhenoCycler, CosMx, and Singular G4X use oligonucleotide-barcoded antibodies combined with cyclic fluorophore targeted imaging to achieve spatially resolved, multiplexed protein detection. These approaches require highly specific antibody sets that are compatible for co-hybridization. In contrast, the COMET platform applies only two label-free primary antibodies at a time, with iterative staining and elution, thereby mitigating potential cross-reactivity and steric hindrance. IMC, a mass spectrometry-based method, uses antibodies conjugated to metal isotopes and detects proteins via laser ablation and time-of-flight mass spectrometry, avoiding spectral overlap but operating at slightly lower spatial resolution (~1 μm) compared to optical imaging-based platforms. While spatial proteomics technologies are advancing rapidly, improvements in antibody validation across tissue types, robust and scalable panel design, and more efficient multiplexing strategies will be essential for broadening their utility and clinical applicability.

Spatial metabolomics

Spatial metabolomics maps small molecules, including metabolic intermediates, lipids, glycans, and small peptides, directly onto tissue sections. This is typically achieved through surface ionization and laser ablation techniques, often with distinct ionization strategies tailored to the chemical properties of specific analytes (Figure 1C). Matrix-Assisted Laser Desorption/Ionization Imaging Mass Spectrometry (MALDI-IMS)⁴⁸ is among the most established and commonly used modalities of mass spectrometry imaging (MSI) in spatial metabolomics. Following the application of a chemical matrix to facilitate ionization, MALDI-IMS acquires spatially resolved mass spectra from intact tissue sections and supports both untargeted and targeted detection of a wide range of metabolites. It typically achieves spatial resolutions of 10–50 µm. Other emerging MSI techniques include desorption electrospray ionization (DESI)⁴⁹ and secondary ion mass spectrometry (SIMS),⁵⁰ which offer complementary capabilities. DESI uses a charged solvent spray for ambient ionization and requires minimal sample preparation, making it suitable for rapid clinical applications. In contrast, SIMS employs a focused ion beam to sputter and ionize molecules from the tissue surface, providing submicron spatial resolution but more limited molecular coverage. Recent advances, such as the timsTOF flex MALDI-2 (Bruker),⁵¹ which combines post-ionization with ion mobility separation, are enhancing sensitivity and expanding metabolite coverage in spatial metabolomics. Ongoing improvements in ionization efficiency, metabolic coverage, and spatial resolution are further enhancing the utility of spatial metabolomics, offering unique opportunities to investigate metabolic gradients and their clinical relevance.

Next-generation innovations in spatial omics

By integrating the strengths and compensating for the limitations of individual spatial omics modalities, recent innovations have enabled the development of integrated platforms that can simultaneously or sequentially profile multiple molecular layers^{40,52,53} from the same tissue section. In parallel, emerging three-dimensional (3D) spatial technologies^{54–56} are enhancing our ability to study tissue architecture in depth, providing new insights into spatial organization across volume and scale.

Same-section spatial multi-omics

Several spatial multi-omics platforms have now been developed to jointly profile distinct molecular features from a single tissue section (Figure 1D). Spatial CITE-seq⁵⁷ extends the standard CITE-seq workflow by integrating antibody-derived tags (ADTs) and mRNA capture with spatial barcoding on slides or beads, enabling simultaneous detection of RNAs and surface proteins at near single-cell resolution (typically 10–25 µm). Similarly, combined with CITE-seq, the Stereo-CITE Proteo-Transcriptomics Set (STOmics) enables simultaneous detection of the whole transcriptome and over 100 proteins on the same tissue section. DBiT-seq⁴⁰ enables co-mapping of mRNAs and proteins via orthogonal microfluidic barcoding directly applied to tissues, achieving ~20 µm resolution. A recent variant, Patho-DBiT,⁵⁸ adapts this workflow for clinical FFPE tissues by incorporating *in situ* polyadenylation, enabling whole-transcriptome sequencing and spatial profiling of gene expression, RNA processing, splicing isoforms, non-coding RNAs, and spatial single-nucleotide variants (SNVs). Vicari et al.⁵² developed a multi-omic approach that combines spatial

transcriptomics, MSI, and histology on the same tissue section, enabling co-mapping of transcriptomes and metabolomes while preserving tissue morphology. Xenium supports same-section multi-omics using targeted gene panels (<500 genes) and a 27-marker protein subpanel. COMET enables simultaneous spatial detection of RNA and protein by combining RNAscope Hi-Plex Pro with sequential immunofluorescence (seqIF) using off-the-shelf, non-conjugated primary antibodies.

In addition to simultaneous detection, several platforms support sequential multi-omics from the same tissue section. For example, the PhenoCode Discovery IO60 Human Protein panel can be performed post Xenium 5K on the same tissue section. CosMx WTX can be followed by multiplexed protein detection of up to 64 targets. Singular G4X enables spatial profiling of ~350 genes, followed by the detection of 15 proteins and fluorescent H&E staining. Direct TCR/BCR sequencing can be performed on serial sections. Takei et al. recently introduced two-layer seqFISH+,⁵³ a high-resolution spatial genomics platform that integrates the mapping of over 100,000 genomic loci and nascent transcripts from ~18,000 genes with subnuclear structural imaging, allowing analysis of genome organization and transcriptional activity within individual cells. These same-section multi-omic approaches preserve spatial context while expanding molecular insight, making them especially valuable in clinical settings with limited samples and critical for overcoming challenges of integrating multimodal data across serial sections.

Spatial 3D technologies

Advancing from 2D to 3D spatial molecular profiling marks a transformative leap in cancer research, opening new avenues for improving cancer diagnosis and treatment.⁵⁹ In general, 3D spatial molecular profiling can be achieved either through serial-section reconstruction^{55,56,60,61} or via non-disruptive volumetric imaging approaches^{62–64} (Figure 1E). The serial-section approach involves iterative serial sectioning followed by molecular profiling (e.g., transcriptomics, proteomics, genomic alterations) of each section, with image co-registration used to reconstruct 3D models. Recent studies^{55,56,60} have demonstrated its application in the spatial 3D mapping of genomic alterations, tumor clonal structures, and morphological and molecular gradients in human cancers and precursors, providing novel insights into spatial tumor heterogeneity and evolution. Commercial platforms such as those from Singular Genomics enable 3D spatial multi-omic profiling across serial sections of a tissue block, with automatic cell type annotation and 3D niche detection.

Unlike serial-section reconstruction, non-disruptive volumetric methods preserve tissue integrity and include tissue-clearing and permeabilization techniques,^{56,65} which enable deep tissue staining and imaging with confocal or light-sheet microscopy as well as label-free phase imaging.^{62,64,66} Cyclic immunofluorescence (CyCIF), combined with confocal microscopy, proposed as 3D CyCIF, has been used to achieve highly multiplexed 3D profiling of cell states and immune niches in thick tissue.⁶⁴ Commercial light-sheet microscopy systems include the 3Di microscope (Alpenglow Biosciences), a hybrid open-top, light-sheet microscope (OTLS) designed for high-resolution 3D imaging. A recent study demonstrated the combined use of TO-PRO-3 Iodide (TP3, a fluorescent nuclear stain) and eosin (a cytoplasmic/extracellular stain) on human FFPE tissues, followed by clearing, for high-throughput volumetric imaging and

multi-scale 3D pathology using OTLS.⁶⁶ These innovations have been applied to larger clinical specimens.^{63,67} The PaintScape platform (Bruker) utilizes jebFISH, a highly multiplexed *in situ* genome labeling technology combined with microscopic imaging, to directly visualize the 3D genome and generate high-resolution spatial maps of genome organization and chromosomal structure in individual cells.

Label-free phase imaging techniques, such as holotomography, a tomographic imaging technique that uses refractive-index mapping to quantitatively reconstruct 3D cellular, subcellular, and tissue structures without staining or physical sectioning.⁶² Commercial platforms such as HT-X1 and HT-X1-Plus (Tomo-cube) provide high-resolution holotomographic imaging of thick tissue samples and organoid.^{62,68,69} A recent study integrated holotomography with deep learning to generate 3D virtual H&E images from colon and gastric cancer tissue slices up to 120 µm thick, enabling the visualization of subcellular and micro-anatomical structures while preserving tissue integrity.⁶²

As 3D spatial profiling technologies rapidly advance, large collaborative initiatives such as the Human Tumor Atlas Network (HTAN) Phase 2 research centers are spearheading efforts to chart the 3D multimodal landscapes of human tumors and precursors. To fully unlock the potential of these technologies and transform how 3D data are shared, analyzed, and applied in cancer research, it is crucial to establish standardized voxel-based 3D data formats, robust computational pipelines, and visualization tools that enable seamless data integration and interoperability.

ANALYTICAL BREAKTHROUGHS IN TUMOR SPATIAL PROFILING

The tumor ecosystem displays remarkable spatial complexity, driven by cellular heterogeneity and plasticity, clonal evolution, therapy-induced adaptations, and dynamic changes in the TME. Unraveling these complex cellular and molecular architectures in the spatial context requires advanced analytical strategies that go beyond conventional frameworks. Here, we review key computational approaches—ranging from cell segmentation and feature extraction to cell-cell communication, clonal architecture, 3D model construction, and emerging foundation models. We further discuss strategies for integrating multimodal spatial data to achieve a comprehensive understanding of tumor ecosystems (Figure 2).

Key computational approaches

Cell segmentation

Cell segmentation is a fundamental step in spatial data analysis, crucial for precise transcript mapping and accurate cell phenotyping, and it impacts downstream analysis such as cell-cell interactions. The diverse morphologies of tumor, immune, and stromal cells, along with their highly variable spatial organization, pose significant challenges for segmentation algorithms. Most approaches rely on structural markers to delineate individual cells. Single-channel methods, such as StarDist,⁷⁰ typically use nuclear stains (DAPI or H&E) and infer pseudo-cell boundaries through nuclei expansion or Voronoi tessellation, generating pseudo-cell boundaries. In contrast, dual-channel methods, including DeepCell and Cellpose, incorporate both nuclear and

cytoplasmic signals to achieve true cell segmentation. Transcriptomic platforms such as CosMx and Xenium provide marker-specific staining for nuclei, cytoplasm, and cell membrane, and employ fine-tuned segmentation models (e.g., Cellpose or DeepCell) combined with machine learning to improve segmentation accuracy. In addition to staining-based signals, transcript distribution can also inform cell segmentation. Segger,⁷¹ a transcript-aware framework, models spatial relationships between nuclei and surrounding transcripts to refine initial boundaries to improve transcript-to-cell assignment and downstream analyses.

Feature data preprocessing

Proper spatially aware data preprocessing, including noise correction, normalization, and dimensionality reduction, is essential for downstream analyses. During *in situ* RNA detection or tissue processing, RNA molecules may diffuse to neighboring regions or be incorrectly assigned to adjacent cells. For spot-based platforms, SpotClean⁷² and BayesTME⁷³ employ probabilistic spatial kernels to infer and correct contamination from neighboring spots, while SPLIT⁷⁴ uses snRNA-seq-informed deconvolution to isolate true intracellular signals and reduce diffusion-induced noise. For subcellular resolution platforms, Segger⁷¹ learns transcript-cell relationships to reassign misplaced RNAs. Because spatial data captures local variations in cell density and composition, preprocessing should correct technical variation while preserving true biological heterogeneity. SpaNorm,⁷⁵ using a generalized linear model, decomposes variation into biological and technical components and applies location-specific scaling factors to remove technical noise without disrupting spatial patterns. SpatialPCA⁷⁶ extends probabilistic PCA by incorporating spatial coordinates through a location-based kernel, ensuring that inferred low-dimensional factors vary smoothly across neighboring spots and retain spatial domain structure.

Resolution enhancement, feature expansion, and cell reconstruction

Beyond standard platform features, various tools enhance data by increasing spatial resolution or incorporating additional features for downstream analysis. SpaGCN⁷⁷ leverages graph convolutional networks (GCNs) to jointly model gene expression, spatial adjacency, and histological information to refine spatial clustering. TESLA⁷⁸ applies self-representation learning with GCNs to divide each low-resolution spot into multiple virtual sub-spots using information from neighboring spots. iSTAR⁷⁹ employs a hierarchical transformer model to extract histological features and associate them with gene expression patterns, enabling the imputation of gene expression from spot level to pixel level across both barcoded and non-barcoded regions. Building on methods that align histological features to refine spatial units, image data from many spatial platforms can be fed into foundation models, such as UNI⁸⁰ for H&E images and KRONOS⁸¹ for fluorescence images, to extract representative features. These features can then be integrated with spatial transcriptomic data to improve the resolution and biological accuracy of spot-, bin-, and cell-level analyses. In addition to resolution enhancement, reconstructing subcellular-resolution data into cell-level transcriptomes can be beneficial. For platforms such as Visium HD, the smallest spatial unit is a 2-µm bin, which typically represents only a fragment of a cell and thus contains sparse information. By contrast, reconstructing these bins into cell-level transcriptomes yields more informative

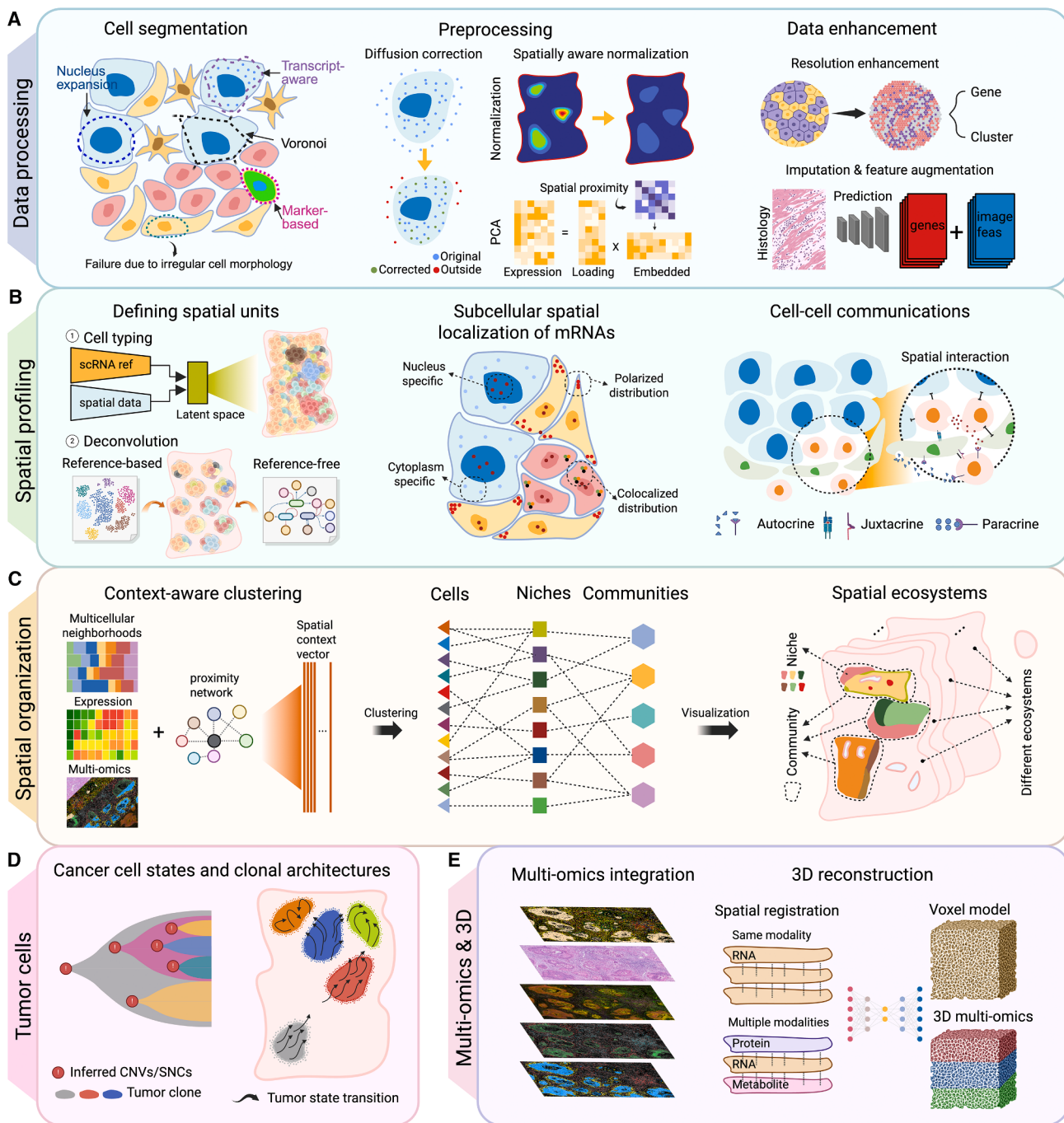


Figure 2. Computational tools and analytical frameworks for spatial omics

(A) Data processing: cell segmentation (left); data preprocessing, including normalization and harmonization (middle); and data enhancement, such as resolution upscaling and feature augmentation (right).

(B) Single-cell/subcellular analysis: defining spatial units via clustering or cell type annotation (left); subcellular spatial localization of mRNAs (middle); and spatially resolved cell-cell communication inference (right).

(C) Spatial organization and ecosystems: context-aware clustering of spatial units (left); hierarchy across scales: from individual cells to spatial niches and communities (middle); and spatial ecosystems (right).

(D) Spatially resolved tumor evolution.

(E) Multimodal integration (left) and volumetric 3D model reconstruction (right).

and biologically interpretable data. Bin2cell⁸² reconstructs individual cells by aggregating bins with similar gene expression profiles and spatial proximity. Extending this concept, SMURF⁸³ models both spatial continuity and gene expression to reconstruct high-confidence single-cell transcriptomes from high-resolution data.

Cell phenotyping and deconvolution

Spatial platforms vary in resolution, necessitating either cell phenotyping (for single-cell data) or deconvolution (for spot-level data) to profile the spatial cellular landscape. Most platforms that provide single-cell features have limited gene coverage, constraining conventional cell phenotyping approaches developed for single-cell RNA sequencing (scRNA-seq). To address this, methods such as Spatial-ID⁸⁴ leverage transfer learning and spatial embedding to integrate reference scRNA-seq data with spatial transcriptomics, achieving improved cell typing accuracy. STANN⁸⁵ applies a deep neural network model to map cell types from scRNA-seq to single-cell spatial data, while BANKSY⁸⁶ combines per-cell molecular profiles with neighborhood context to enable cell phenotyping informed by tissue architecture and the microenvironment.⁸⁶ For deconvolution, methods such as RCTD,⁸⁷ SPOTLight,⁸⁸ cell2location,⁸⁹ Tangram,⁹⁰ Cytospace,⁹¹ and Spotiphy⁹² estimate cell-type composition at the spot or pixel level using reference scRNA-seq data. In contrast, ScType⁹³ and Celloscope⁹⁴ operate without single-cell references, instead relying on curated gene signature panels.

Spatial subcellular analysis

Advances in spatial omics now enable molecular profiling at subcellular resolution. Distinct spatial transcript distribution patterns within a cell, such as distance from the nucleus or cell centroid, polarization, spatial entropy, and cluster dispersion, provide insights into key biological processes, including mRNA trafficking, subcellular organization, and functional heterogeneity. TopACT⁹⁵ applies topological data analysis to extract multi-scale spatial features from subcellular transcript distributions, enabling refined cell state classification. Similarly, CellSP,⁹⁶ Bento,⁹⁷ and PHOTON⁹⁸ identify spatially coherent gene modules within single cells, revealing previously unrecognized layers of subcellular heterogeneity.

Cell-cell communication

Deciphering the molecular dialogues between neighboring cells is fundamental to understanding how cellular communities coordinate behaviors, shape tissue organization, and drive tumor-immune interactions within the TME. Spatial transcriptomics uniquely enables the direct mapping of these interactions *in situ*, linking ligand-receptor signaling to the spatial context and overcoming key limitations of scRNA-seq. Widely used single cell-based communication methods, such as CellPhoneDB⁹⁹ and CellChat,¹⁰⁰ now have spatially adapted versions that restrict ligand-receptor (LR) interactions to spatially adjacent cells. Giotto,¹⁰¹ SOAPy,¹⁰² Squipy,¹⁰³ Spateo,¹⁰⁴ and CytoSignal¹⁰⁵ also provide modules for inferring cell-cell communication by integrating ligand-receptor expression with spatial information, differing primarily in how they quantify LR communication scores. COMMOT¹⁰⁶ leverages optimal transport to model the cost-efficient flow of signaling molecules between cell types based on spatial proximity. NCEMs¹⁰⁷ and NEST¹⁰⁸ employ graph-based modeling to capture how a cell's spatial neighborhood influences its gene expression and, in turn, its communication potential.

NicheNet¹⁰⁹ and SpaTalk¹¹⁰ connect secreted ligands to downstream expression changes in target cells, linking spatial signaling to functional outcomes. As spatial technologies rapidly evolve, increasing resolution and gene coverage will enable more precise and comprehensive mapping of cell-cell communication networks.

Spatial cellular niches and communities

Spatial domains can be viewed as spatially co-localized, functionally coordinated groups of cells—often termed multicellular neighborhoods, spatial niches, ecotypes, or communities—reflecting different scales of organization and input features. Because co-localization is a defining characteristic, the composition of neighboring cells (commonly defined by nearest neighbors, cells within a certain distance, or Delaunay triangulation, as implemented in Giotto¹⁰¹ and Squipy¹⁰³) is frequently used to identify distinct cellular neighborhoods.¹⁴ UTAG¹¹¹ integrates gene expression from central and neighboring cells to construct spatial proximity graphs, which is then used to infer niche clusters via Leiden clustering. CellCharter¹¹² extends this approach by incorporating multi-omics data into the spatial graph and applying a Gaussian mixture model to identify spatial niches from the learned latent representations. Building on this, scNiche¹¹³ integrates additional features such as neighborhood cell composition and image-derived features to construct refined spatial proximity graphs. NicheCompass¹¹⁴ further incorporates prior knowledge of interacting pathways into its embedding framework and replaces the standard dot-product decoder with a cosine similarity-based decoder to improve the accuracy of spatial proximity learning.

Spatial mapping of cancer cell states

Elucidating how distinct cancer cell states are spatially organized and how they interact with microenvironmental cues is crucial for understanding cancer progression. Trajectory inference tools such as Monocle3,¹¹⁵ scVelo,¹¹⁶ Slingshot,¹¹⁷ CellRank,¹¹⁸ and CytoTRACE¹¹⁹—originally developed for scRNA-seq—have been adapted to infer pseudo-temporal trajectories within tissue sections. Spateo¹⁰⁴ extends RNA velocity analysis into 2D and 3D contexts, enabling the reconstruction of cellular trajectories and processes such as tumor evolution within native tissue architectures. The PSTS model from stLearn¹²⁰ integrates gene expression dynamics (pseudotime) with spatial proximity to infer spatiotemporal trajectories. Similarly, TopoVelo¹²¹ combines spatial information with RNA velocity in a graph-based framework, allowing the reconstruction of spatiotemporal cell state transitions across tissues.

Spatially resolved genomic alterations and clonal architecture

Spatially resolving copy number variations (CNVs) and mutations is critical for elucidating tumor evolutionary dynamics. While SNVs and CNVs are traditionally called from DNA sequencing, they can now be inferred from spatial transcriptomic data. Tools such as inferCNV,¹²² HoneyBADGER,¹²³ CopyKAT,¹²⁴ STARCH,¹²⁵ SCmut,¹²⁶ scSNV,¹²⁷ and SComatic,¹²⁸ originally developed for single-cell analysis, have been adapted for the spatial context. For instance, SpatialInferCNV¹²⁹ integrates inferCNV into a customized pipeline for spot-level spatial transcriptomics data, enabling phylogenetic reconstruction based on CNV profiles.^{129,130} stSNV¹³¹ leverages the SComatic tool to generate a comprehensive map of spatially resolved SNVs from spatial transcriptomics data. Although inferred CNVs and clonal architecture

Box 1. Horizontal, vertical, and diagonal spatial data integration

Horizontal integration (same modality, *different samples/sections*).

- **Anchor:** shared features (genes/proteins/metabolites).
- **Goal:** remove batch effects, pool power, compare groups.
- **Tactics:** batch correction and joint embedding with spatial awareness (e.g., models that preserve neighborhoods/domains).
- **Pitfalls:** over-correction of true biological differences; uneven ROIs across samples.

Vertical integration (multiple modalities on the same section/ROI).

- **Anchor:** shared spatial units (cells/spots/voxels/ROIs).
- **Goal:** co-localize signals (e.g., RNA-protein), cross-modal imputation, pathway synthesis.
- **Tactics:** shared segmentation, fiducials for channel alignment, per-pixel registration, joint QC.
- **Pitfalls:** misregistration, signal bleed/antibody crosstalk, scale mismatch (counts vs. intensities).

Diagonal integration (different modalities on *different sections/samples*).

- **Anchor:** weak linkages—morphology, landmarks, cell/state dictionaries, or learned cross-modal embeddings.
- **Goal:** fuse complementary assays when co-assay is not possible.
- **Tactics:** image co-registration, optimal-transport/graph matching, contrastive learning with shared features.
- **Pitfalls:** sectioning offsets, platform bias, non-overlapping biology; requires uncertainty reporting.

generally align with those derived from DNA sequencing, orthogonal validation remains important to ensure accuracy.

Image co-registration and 3D model construction

Constructing 3D models of tissues typically requires volumetric data acquisition, which can be achieved through either destructive or non-destructive approaches. Non-destructive methods derive 3D information from intact tissues using techniques such as optical sectioning (confocal/light-sheet microscopy), volumetric imaging of cleared tissues, or computational inference. In contrast, destructive methods involve serial physical sectioning, where each section is individually imaged and digitally registered to reconstruct the 3D volume. Lin et al.⁵⁶ developed a CyCIF-based pipeline for high-resolution 3D reconstruction of cellular and organelle-level structures. The CODA¹³² framework enables 3D reconstruction from serial H&E-stained sections, capable of integrating molecular and mutational data.⁵⁵ A recent study by Mo et al. demonstrated successful co-registration of large numbers of serial Visium sections to investigate 3D tumor progression and clonal dynamics.⁵⁴

Foundation models

With the rapid expansion of digitalized histology and spatial omics data, several foundation models (FMs) have emerged for spatial data analysis and integration. In the histology-centric category, multiple FMs, including UNI⁸⁰ provide pretrained histopathology encoders that serve as powerful backbones for downstream spatial and molecular tasks. In the histology image-omics integration category, models such as LOKI,¹³³ which uses contrastive language-image pretraining, align H&E histology with spatial transcriptomics to enable zero-shot tasks, including spatial alignment, cell-type decomposition, clustering, and cross-modal retrieval. In parallel, GigaTIME,¹³⁴ a multimodal AI framework for generating virtual mIF from H&E images, and deep-learning frameworks, such as ROSIE,¹³⁵ built on a modern ConvNeXt convolutional architecture, computationally infer the expression and spatial localization of dozens of proteins from H&E images. While not strictly an FM, ROSIE exemplifies the growing class of histology-to-molecule prediction approaches that are increasingly relevant to cancer spatial omics. In the omics-centric category, models such as CellPLM,¹³⁶ scGPT-spatial,¹³⁷ NicheFormer,¹³⁸ and KRONOS⁸¹ leverage transformer architec-

tures,¹³⁹ whereas models such as Novae leverage graph-based architectures, to capture generalizable biological features across diverse tissue types and experimental conditions. These models support a broad spectrum of downstream tasks, including cross-platform integration, spatial domain identification, gene expression imputation, and prediction of cell types and cell-cell interactions. Their versatility and scalability make them powerful tools for enhancing the interpretability and robustness of spatial data, particularly in settings where direct measurements are sparse or noisy. As these approaches continue to evolve, they hold promise for uncovering hidden spatial biology and accelerating translational discovery in cancer.

Multimodal spatial data integration

Spatial data vary in resolution, panel design, and feature types (e.g., RNA, protein, or metabolite), creating significant challenges for data integration—a critical step toward deriving unified biological insights (Box 1).

Integrating data from the same spatial profiling platform

When integrating spatial datasets derived from the same platform, the process resembles batch correction, for which numerous methods established in single-cell analysis, including WNN, CCA, RPCA, and Harmony, are commonly applied. However, when datasets exhibit spatial dependency across samples, spatial-aware integration methods should be used to preserve tissue architecture. PASTE¹⁴⁰ integrates multiple spatial transcriptomics datasets by jointly modeling spatial structure and gene expression using a probabilistic optimal transport framework, while STAligner¹⁴¹ performs integration through graph-based spatial representation learning.

Cross-platform spatial data integration

Integrating datasets from different spatial platforms requires reconciling differences in resolution, feature space, and tissue coverage. A common strategy is to co-embed shared features into a unified latent space. SpaMosaic¹⁴² leverages graph neural networks and contrastive learning on spatial and molecular graphs to generate a co-embedding across modalities. When datasets originate from adjacent sections or matched samples, spatial information can further guide integration. SpaMTP¹⁴³ aligns and analyzes spatial metabolomics and transcriptomics

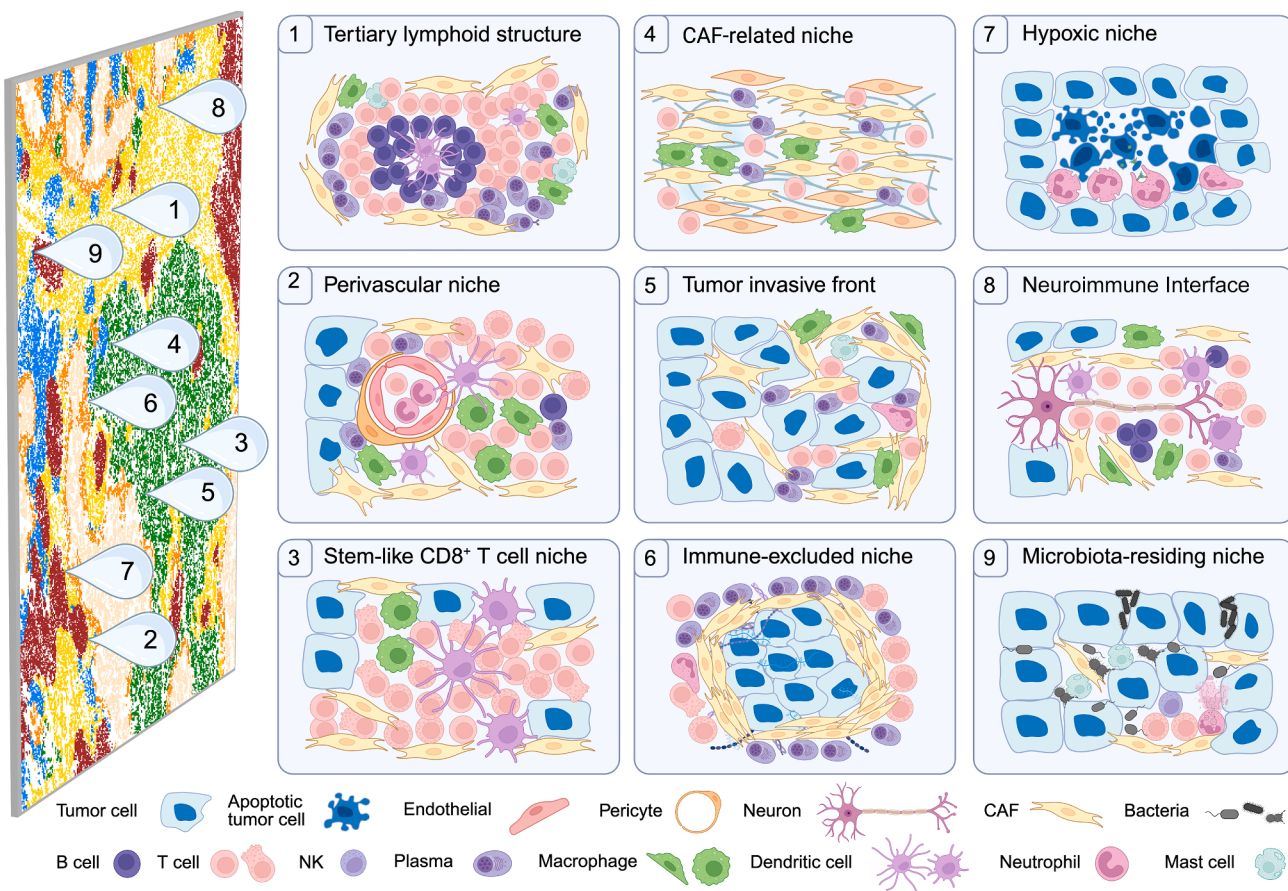


Figure 3. Spatial mapping of TME niches

Schematic illustrates the characteristic cellular composition and organization of nine biologically important spatial niches within the tumor microenvironment.

in a coordinated manner. MISO¹⁴⁴ integrates multiple omics layers, including molecular and histological modalities collected from the same spatial grid, by constructing modality-specific spatial graphs and embedding them with neural networks. Moving forward, cross-cohort multimodal data integration—linking spatial datasets across platforms, tissue types, and cohorts—remains a major challenge. Foundation models trained on large, diverse datasets offer a promising avenue for addressing this by learning generalizable features that facilitate integration and construction of comprehensive spatial cancer atlases.

UNRAVELING TUMOR MICROENVIRONMENT COMPLEXITY

The TME is a highly heterogeneous and dynamic ecosystem composed of immune and stromal populations in diverse states, along with extracellular matrix components, all spatially organized and evolving during tumor progression and therapy response. Spatial omics technologies extend beyond single-cell profiling to map how cellular niches, their spatial organization, and crosstalk with cancer cells drive immune evasion and tumor evolution. Importantly, *in situ* profiling is less prone to cell-capture bias than dissociation-based methods, faithfully capturing cellular compositions and facilitating the detection of rare or fragile cell

types and states, with benefits further enhanced by the substantially higher throughput of spatial omics. This section highlights key advances in the spatial profiling of the TME, with a particular focus on cellular organization and interactions within functional niches, their underlying biology, and their emerging potential as therapeutic targets and predictive or prognostic biomarkers.

Mapping functional niches in the tumor microenvironment

The TME is organized into spatially distinct cellular niches with profound biological and clinical relevance. Yet, their spatial architecture and functional dynamics remain incompletely understood. Spatial profiling technologies now provide a powerful means to uncover recurring and context-specific niches. Leveraging these advances, recent studies have revealed diverse functional niches characterized by unique cellular organization, communication networks, and molecular signatures (Figure 3).

1. **Tertiary lymphoid structures (TLSs):** TLSs are extensively studied spatial structures, known for orchestrating local B cell-mediated antitumoral immunity and correlating with favorable clinical outcomes.^{145,146} Spatial profiling has enabled detailed characterization of TLS distribution,

maturation states, and functional roles. In renal cell carcinoma (RCC),¹⁴⁷ TLSs function as sites of *in situ* B cell maturation toward plasma cells. These plasma cells migrate along CXCL12⁺ fibroblastic tracks and disseminate into the tumor bed, where, in patients treated with immune checkpoint inhibitors (ICIs), IgG deposition on tumor cells correlates with malignant cell apoptosis, higher response rates, and prolonged survival.¹⁴⁷ Beyond RCC, spatial studies across cancers have further dissected TLS-associated TME features and their clinical relevance. In gastric cancer, TLSs located in the tumor core were enriched with CD8⁺ T cells, particularly those expressing PD-1 but not TIM-3, a phenotype that correlated with improved survival.¹⁴⁸ In nasopharyngeal cancer, CXCL13⁺ CAFs and CXCL13⁺CD8⁺ T cells co-localize with B cell aggregates within TLSs, where CXCL13⁺ CAFs promote B cell adhesion and antibody production, and plasma cell-derived antibodies induce the apoptosis of EBV-positive malignant cells.¹⁴⁹ In breast cancer, TLS regions contain diverse cell types, including two fibroblast subsets (CCL21⁺ and APOD⁺) that recruit T and B cells via the CXCL12–CXCR4 axis.¹⁵⁰ Recent efforts also focus on factors influencing TLS formation and maturation. In high-grade serous ovarian cancer, TLS formation and activity vary across anatomical sites and may be suppressed by cancer-educated mesenchymal stem cells.¹⁴⁵ In hepatocellular carcinoma, TLS maturation trajectories have been reconstructed, classifying immature TLSs as conforming or deviating subtypes, and tumor-derived tryptophan metabolites were found to impair TLS maturation.¹⁵¹ However, most studies involve small cohorts and lack longitudinal sampling. Systematic efforts to track TLS cellular dynamics, maturation trajectories, and functional states over time are needed to identify factors that arrest TLS maturation or drive TLS dysfunction.

2. **Perivascular niches** Perivascular niches, organized around tumor blood vessels (Figure 3), serve as critical hubs for coordinating local immune responses. These niches support dendritic cell (DC)-T cell interactions for antigen presentation and local T cell priming, facilitating effective antitumoral immunity.¹⁵² Within these niches, DC-T cell clusters are frequently positioned adjacent to endothelial and stromal cells, whereas macrophages and regulatory populations often localize at the outer boundary, forming a layered architecture that shapes the local immune context. Chemokine gradients (e.g., CCL19/21-CCR7, CXCL12-CXCR4) orchestrate the recruitment of both effector and immunosuppressive immune populations. The balance between effector cell recruitment and suppressive cell accumulation ultimately dictates whether the niche promotes antitumoral immunity or fosters immune exclusion.¹⁵³ Spatial profiling has enabled high-resolution mapping of vascular-stromal-immune crosstalk within these niches. A study in glioblastoma (GBM) revealed a collagen-rich ECM rim as a dominant feature of perivascular niches in recurrent tumors.¹⁵⁴ These niches were enriched with immunosuppressive macrophages, glia, and collagen-producing stromal cells, suggesting therapy-driven remodeling of the perivascular microenviron-

ment. Another glioma study reported perivascular niches enriched not only with microglia and macrophages but also with B cells, highlighting their broader immunological complexity.¹⁵⁵ In hepatocellular carcinoma (HCC), IMC identified VEGFA⁺ macrophages within perivascular niches, engaging in VEGFA-mediated interactions with CD34⁺ endothelial cells, contributing to an immune-regulatory microenvironment.¹⁵⁶

3. **Stem-like CD8⁺ T cell niches** Stem-like CD8⁺ T cells, characterized by the high expression of *TCF1* and *CD28* and the absence of terminal exhaustion markers (e.g., TIM-3), form specialized niches in close association with antigen-presenting cells (APCs).¹⁵⁷ Within these niches (Figure 3), stem-like CD8⁺ T cells act as a self-renewing reservoir, maintaining proliferative capacity and undergoing asymmetric division to replenish the effector pool while preserving a stem-like subset.¹⁵⁸ This process, central to sustaining antitumoral immunity, is supported by epigenetic reprogramming, CXCR6 upregulation, and crosstalk with cDCs via CXCL9, IL-15, and CCR7-binding chemokines (CCL19 and CCL21), along with additional co-stimulatory and cytokine inputs that sustain the stem-like pool and drive effector differentiation.^{159–161} The presence of these niches is closely linked to clinical responses to immune checkpoint blockade (ICB),¹⁶² whereas their absence may contribute to tumor immune evasion.¹⁵⁷ Activation of DCs through FLT3L or CD40 has been shown in preclinical models to expand these niches,^{163–165} suggesting a potential strategy that could complement ICB. Spatial multimodal analyses offer high-resolution insights into the cellular organization and signaling networks governing the formation, maintenance, and therapeutic remodeling of these niches, highlighting their potential as biomarkers for patient stratification.
4. **CAF-related niches** Cancer-associated fibroblast (CAF)s are highly heterogeneous, differing in cellular origins, phenotypic states,^{166–168} and functions. Their plasticity and context dependence pose challenges for studying CAF biology. Single-cell and spatial analyses have revealed that CAFs form structurally and functionally distinct niches that shape the immune milieu and therapeutic responses.^{14,169} In many tumors, matrix-producing CAFs generate dense collagen-rich barriers that hinder T cell infiltration and interaction with tumor cells, contributing to immune exclusion.^{167,170,171} Inflammatory CAFs secrete immunomodulatory cytokines and chemokines, such as CXCL12 (SDF-1), IL-6, and TGF- β , shaping immune cell recruitment, polarization, and function.¹⁷⁰ Antigen-presenting CAFs can present antigens to T cells and support antitumor immune responses.^{167,172} Most spatial studies have characterized CAFs by first defining their phenotypes based on marker expression, an approach that can be limited by gene coverage or antibody availability. In a recent pan-cancer spatial multi-omics study, Liu et al.,¹⁴ employed a novel strategy based on neighboring cell composition to define four conserved CAF organizational patterns (s1-s4 CAFs) across cancers. These niches exhibited distinct intercellular communication networks,

refining our understanding of how CAF phenotypes and functions are shaped by microenvironmental interactions, which also influence the abundance and states of immune cells within the niches.¹⁴ Further studies leveraging spatial technologies and functional genomics may deepen our understanding of CAF organization and interactions, providing a foundation for therapeutic modulation.

5. **Tumor invasive front** The tumor invasive front is a dynamic interface where malignant cells engage with stromal and immune components, critically influencing cancer progression and metastasis. Spatial profiling has revealed distinctive cellular compositions and signaling gradients in this region¹⁷³ (Figure 3). This zone often harbors an immunosuppressive microenvironment¹⁷⁴ enriched with tumor-associated macrophages (TAMs), regulatory T cells, and neutrophils, which collectively suppress antitumor immunity. Tumor cells at the invasive front frequently display cell state reprogramming, with tendencies toward stem-like, hypoxic, or therapy-resistant phenotypes.¹⁷⁵ Spatial analyses show that these leading-edge phenotypic changes coincide with an altered immune landscape, reflecting adaptation to evade immune surveillance. Additionally, leading-edge tumor cells often upregulate immune checkpoint molecules, downregulate antigen presentation, and exhibit enhanced migratory and invasive programs—features linked to poor prognosis and immunotherapy resistance across solid tumors.¹⁷⁶
6. **Immune-excluded niches** Immune-excluded niches are tumor regions where lymphocytes, particularly cytotoxic T cells, accumulate at the margin or stroma but fail to infiltrate the parenchyma (Figure 3), a pattern linked to poor responses to ICB. Spatial analyses show these niches are often encapsulated by dense stromal barriers and enriched with immunosuppressive myeloid cells, creating a microenvironment hostile to lymphocyte trafficking. Such patterns are observed across multiple cancer types.^{14,130,177,178} Spatial profiling has begun to dissect the molecular and cellular architecture of these niches, revealing key drivers of immune exclusion, including: (i) physical barriers from dense ECM deposited by CAFs,¹⁷⁷ (ii) chemokine gradients that repel or misdirect lymphocytes, such as the CXCL12-CXCR4 axis,¹³⁰ (iii) immunosuppressive cytokine signaling, notably TGF- β ,¹⁴ and (iv) inhibitory interactions such as CD47-THBS1, which further reinforce immune exclusion. Targeting these factors, for example via TGF- β blockade, has been shown to enhance T cell infiltration and sensitize immune-excluded tumors to ICB,¹⁷⁹ highlighting the therapeutic potential of modulating exclusionary barriers.
7. **Hypoxic niches** Hypoxic niches are metabolically distinct regions where limited oxygen availability drives restructured tissue architecture and phenotypic reprogramming in malignant and stromal cells. These niches are enriched for aggressive tumor cells and immunosuppressive TME subsets (Figure 3). Spatial profiling in GBM revealed organized, layered structures surrounding hypoxic niches, reflecting adaptation to oxygen gradients across tissue zones.¹⁸⁰ Hypoxia correlates with the preferential localization of TAMs displaying proinflammatory and immunosuppressive phenotypes, whereas microglia tend to reside in

normoxic regions.¹⁸¹ In HCC, hypoxia coincides with the induction of SPP1 $^{+}$ TAMs that co-localize with CAFs to drive immune exclusion.¹⁷⁸ Moreover, hypoxia promotes the expression of stemness and chemoresistance programs in quiescent tumor cells.¹⁸² Emerging evidence suggests hypoxic niches foster neutrophil reprogramming toward pro-tumorigenic phenotypes,¹⁸³ reinforcing their role in immune suppression and therapeutic resistance.

8. **Neuroimmune interface** Neural elements are increasingly recognized as active participants in the TME, shaping local immunity through neurotransmitters, neuropeptides, and axon-glia signaling. Spatial profiling has revealed specialized neuroimmune niches (Figure 3) where neural signals modulate immune function, with context-dependent effects ranging from antitumor support to immune suppression.^{184–186} In GBM, myelin damage and lipid debris can engage TREM2 $^{+}$ TAMs, influencing their activation states.¹⁸⁷ In PDAC, recent spatial analyses show that non-invaded nerves are often associated with lymphoid aggregates/TLS,¹⁸⁸ whereas invaded nerves are surrounded by NLRP3 $^{+}$ TAMs and myCAF s , suggesting distinct neuro-immune interactions that may shape both immune landscapes and neural invasion. Spatial multi-omics in 3D may offer a comprehensive view of neuroimmune interactions *in situ*, capturing their spatial organization, linking them to functional outcomes, and unlocking the potential of the neuroimmune interface as a therapeutic axis.
9. **Microbiota-residing niches** Spatial multi-omics enables high-resolution mapping and quantification of microbiota species and their interactions with tumor and TME cells (Figure 3), providing insights into how they influence cancer cell phenotypes and metabolism, modulate the surrounding microenvironment and antitumoral immunity, to shape cancer progression and therapy responses.^{9,189} Microbiota profiling can be performed by probe-based *in situ* detection (e.g., HiPR-FISH¹⁹⁰ and par-seqFISH¹⁹¹), which enables single-cell or subcellular visualization of microbial taxa—including intracellular bacteria—or by sequencing-based spatial metatranscriptomic approaches, which allow co-profiling of microbial and host transcripts within the same tissue section. A previous study incorporated bacteria transcript capture into the Visium workflow, revealing heterogeneous microbiota distribution and showing that bacteria-rich niches were highly immunosuppressive.⁹ Another study used microbial spike-in probes with GeoMx DSP in lung cancer tissues,¹⁹² finding higher bacterial burden in tumor cells than in the TME or adjacent normal tissue; within the tumor, bacterial load correlated with oncogenic pathways such as Wnt- β -Catenin signaling.¹⁹² Additionally, a *Fusobacterium*-residing niche was linked to cancer cell quiescence and chemoresistance.¹⁹³ While intratumoral bacteria often exhibit tumor-promoting roles, species-specific effects matter. For instance, Zhu et al.¹⁹⁴ demonstrated via spatial metabolomics that gut-derived *Akkermansia muciniphila* had antitumor effects by modulating glutamate metabolism. In PDAC, spatial proteomics linked higher bacterial diversity to increased T cell infiltration in “immune-hot” regions.¹⁹⁵ Recent advances now allow

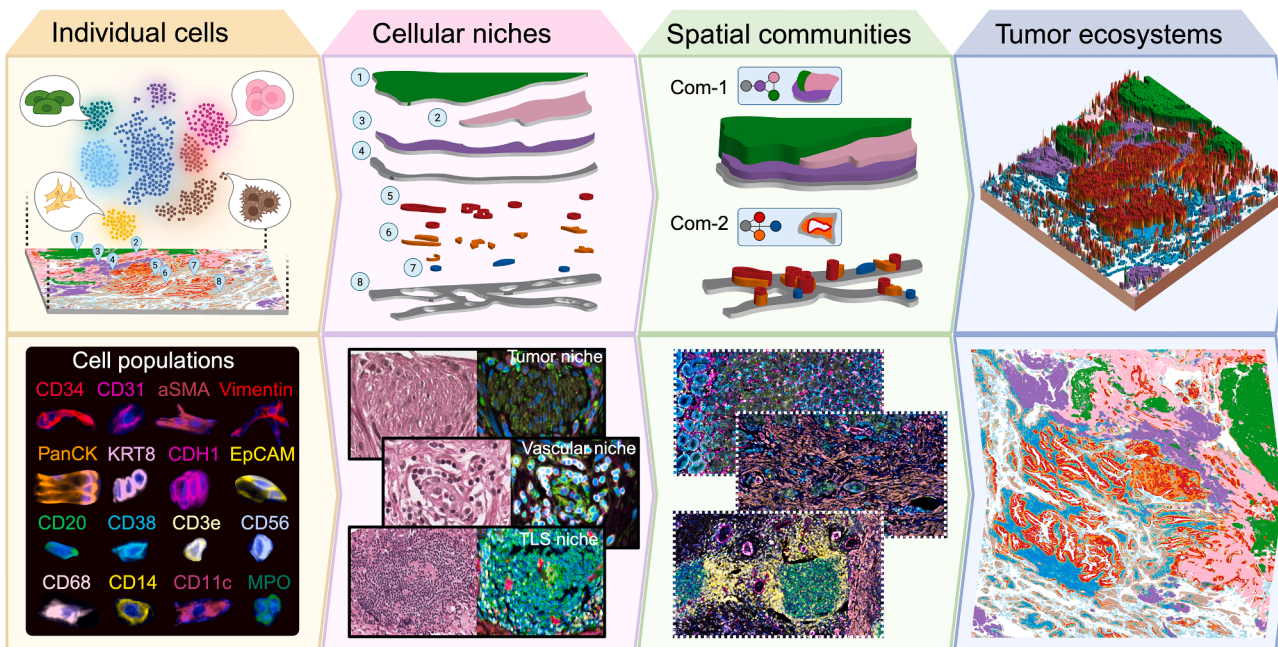


Figure 4. Hierarchy of spatial archetypes across scales

Schematic illustrates the hierarchical organization of spatial archetypes—from individual cells to multicellular niches, spatial communities, and whole-tumor ecosystems.

microbiota-specific probe integration into platforms such as Xenium and CosMx, enabling deeper characterization of microbiome-tumor and microbiome-TME interactions for harnessing microbiota-based therapeutic strategies.

Other spatially organized niches with clinical relevance
Beyond the TME niches described above, several additional spatially organized niches hold significant clinical relevance yet remain poorly characterized. These include: (i) lymphatic niches regulating immune cell trafficking, activation, and cancer cell stemness^{198–200}; (ii) cytotoxic immune niches, where effector cells cluster to mediate antitumor activity but may undergo phenotypic reprogramming^{201,202}; (iii) senescent cell niches enriched in aging- or therapy-induced senescent cells that secrete pro-tumorigenic factors^{203–206}; (iv) pre-metastatic niches, which create permissive microenvironments for circulating tumor cell colonization at distant organs^{207–211}; and (v) metabolically specialized niches, such as regions of metabolic symbiosis,²¹² adipocyte-rich²¹³ microenvironments, and acidotic niches,²¹⁴ that support tumor growth through metabolic adaptations. Spatial multi-omics enables *in situ* characterization of these niches, uncovering their biological functions and therapeutic potential.

From individual cells to tumor ecosystems

Most spatial studies to date have focused on mapping the locations and abundance of individual cell populations or the cellular composition of specific regions. While valuable, this cell-centric view captures only part of the story. Tumors and TME cells are organized into functional niches (Figure 3) that aggregate into high-order spatial communities; together, they form the broader tumor ecosystem (Figure 4; Box 2). Clinically relevant biology

often emerges at these higher organizational levels—specifically, how diverse cell populations are arranged, which partners they repeatedly co-localize with, what signals flow between them, and how these patterns persist or rewire under therapy.

To fully leverage multi-scale spatial profiling, a “zoom-out” perspective is required, necessitating analytical frameworks that explicitly model multicellular organization and dynamics: niche classifiers, community detection, and graph-based models that capture topology, signaling directionality, and resource constraints. Causal and perturbation-aware modeling will be essential for predicting how tumor and TME compartments function as integrated ecosystems and how interventions in one compartment ripple across the entire network. Practically, ecosystem-level biomarkers, such as the abundance of specific niche-community configurations (e.g., a TLS-perivascular community) or the spatial contiguity between functionally distinct regions (e.g., a FAP⁺ CAF rim adjacent to a CD8⁺ T cell-excluded zone; a lactate-rich metabolite gradient co-localizing with TAM accumulation) may ultimately outperform single-cell metrics in predicting prognosis and guiding treatment selection.

CLINICAL AND TRANSLATIONAL APPLICATIONS OF SPATIAL OMICS

Spatial omics is most impactful when anchored in translational studies using well-annotated clinical specimens. Spatial readouts connect patient clinical manifestations and tissue histopathological features to biological mechanisms revealed by cells and molecules captured *in situ*, closing the “bedside-bench-bedsides” loop by turning clinical observations into testable hypotheses and returning actionable biomarkers and targets for patient stratification and precision therapies (Figure 5). In this

Box 2. Spatial hierarchy of tumor ecosystem

- Cell:** An individual cellular unit defined by image-based segmentation.
- Neighborhood:** A small cluster of spatially adjacent cells with recurrent co-occurrence patterns.
- Niche:** A functionally defined microenvironment (e.g., TLS) where specific cell types and cues support specialized behaviors.
- Community:** A higher-order assembly of interacting niches and neighborhoods forming a coherent functional module.
- Region:** A meso-scale compartment demarcated anatomically or histologically (e.g., tumor core, invasive front, peritumor stroma); assigned by pathology or computational segmentation/clustering.
- Zonation:** A structured gradient of cell states or gene programs across space (e.g., hypoxia, metabolic axes).
- Ecotype:** A recurring, cross-sample multicellular composition/state of the TME (often platform-agnostic).
- Archetype:** A canonical interaction pattern (e.g., DC-T cell priming hub) capturing coordinated multivariate features.
- Tumor ecosystem:** The whole-tumor context integrating all communities, regions, and broader exogenous influences.

section, we outline key considerations for incorporating spatial omics into clinical and translational study design—including practical hurdles in sample processing, assay standardization, and analytics—and provide a more structured roadmap for the clinical adoption of spatial technologies. Here, we review the applications of spatial omics in studying precancer biology and interception, cancer metastasis, minimal residual disease (MRD), and novel biomarker and target discovery (Figure 5A).

A roadmap for adopting spatial omics into clinical practice

Integration of spatial-omics assays into clinically oriented studies requires proper planning from the conceptualization phase. Effective clinically oriented spatial studies must begin with the clinical questions to be tackled and the priority clinical endpoints, along with the clinical sampling framework (sampling procedures, time-points, organ sites, turnaround time, and specimen preservation techniques). These factors guide translational study design while simultaneously imposing constraints on spatial assays, which must be considered when selecting optimal profiling platforms and data modalities (Figure 5B). Subsequently, spatial analysis of tumor samples should closely align with the central clinical theme, establishing correlations between cellular or molecular characteristics and clinical parameters, such as tumor stage, metastatic timing and sites, therapeutic response or resistance, and patient prognosis. These correlations will then be translated into deeper mechanistic insights and causal relationships in pre-clinical studies, leading to further development of novel biomarkers or therapeutic strategies for future clinical trials. Thus, continuous crosstalk among clinical, translational, and pre-clinical research teams shapes the roadmap, leading to innovations that keep improving clinical patient management.

As a practical example, in a recent study from our group,²¹⁵ we applied CODEX to baseline and on-treatment tumor samples from patients with recurrent ovarian clear cell carcinoma receiving combination ICB. Spatial profiling revealed a distinct TME landscape and dynamic immune remodeling in tumors harboring *PPP2R1A* loss-of-function mutations, including higher densities of B cells, particularly proliferating and germinal-center-like B cells, and peritumoral secondary follicle-like TLSs, which were associated with improved survival in this subgroup. These spatially resolved findings suggested that the pharmacologic modulation of the PP2A pathway (for which *PPP2R1A* encodes a scaffold subunit) might recapitulate this immune-permissive state more broadly. Based on this mechanism, a hypothesis-

driven clinical trial was initiated to evaluate dostarlimab (PD-1 inhibitor) in combination with the PP2A inhibitor LB-100 in patients with *PPP2R1A*-wildtype ovarian cancer (NCT06065462).

Looking ahead, spatial maps have the potential to become directly actionable in the clinic. For example, spatially resolved immune architectures, such as the presence of TLSs at different maturation states, patterns of immune-stromal interaction, especially T cell exclusion, or niche-specific exhaustion programs, could guide the selection of immunotherapy combinations or identify patients more likely to benefit from therapies that modulate TLS formation or stromal-immune organization (e.g., CXCL13-CXCR5 signaling modulators or CAF-targeting agents). Spatial gradients of hypoxia, metabolism, and vasculature could inform radiation planning or optimize the development of hypoxia-activated prodrugs, while spatially defined tumor cell states or evolutionary patterns may help distinguish patients best suited for neoadjuvant versus adjuvant targeted or ICB therapies. Spatial analysis may also support adoptive cell therapies, such as CAR-T, TIL, or TCR-T, by linking engineered T cell localization and niche-specific interactions with therapeutic efficacy and toxicity, and integrating spatial omics with drug-distribution measurements may reveal intratumoral regions of inadequate drug penetration that contribute to resistance. Although highplex spatial multi-omics remains costly and not yet scalable for routine use, these discoveries can be distilled into low-plex mIF panels that capture key spatial biomarkers, and AI-powered models trained on spatially annotated datasets and routine H&E images may eventually enable the detection of clinically relevant spatial features directly from standard digital pathology, further lowering the barriers to clinical implementation.

Along the roadmap, however, a few key aspects require special considerations, which we detail later in discussion.

Specimen scale influences translational study approaches: Large surgical resections enable ecosystem-scale mapping via multi-region sampling, broader fields of view, multi-omics on the same or adjacent sections, and 3D reconstructions through serial-sectioning or non-disruptive volumetric imaging. Conversely, small tissue biopsies (fine-needle or core-needle) offer limited architectural context but are valuable for target gene/protein readouts, paired baseline/on-therapy comparisons, and rapid validation of spatial biomarkers. Careful region of interest (ROI) selection is critical to mitigate sampling bias. Tissue microarrays (TMAs, 1.5–2 mm cores) retain meso-scale architecture and contain thousands of cells, providing a cost-effective way to validate markers across hundreds of cases for robust correlative studies.

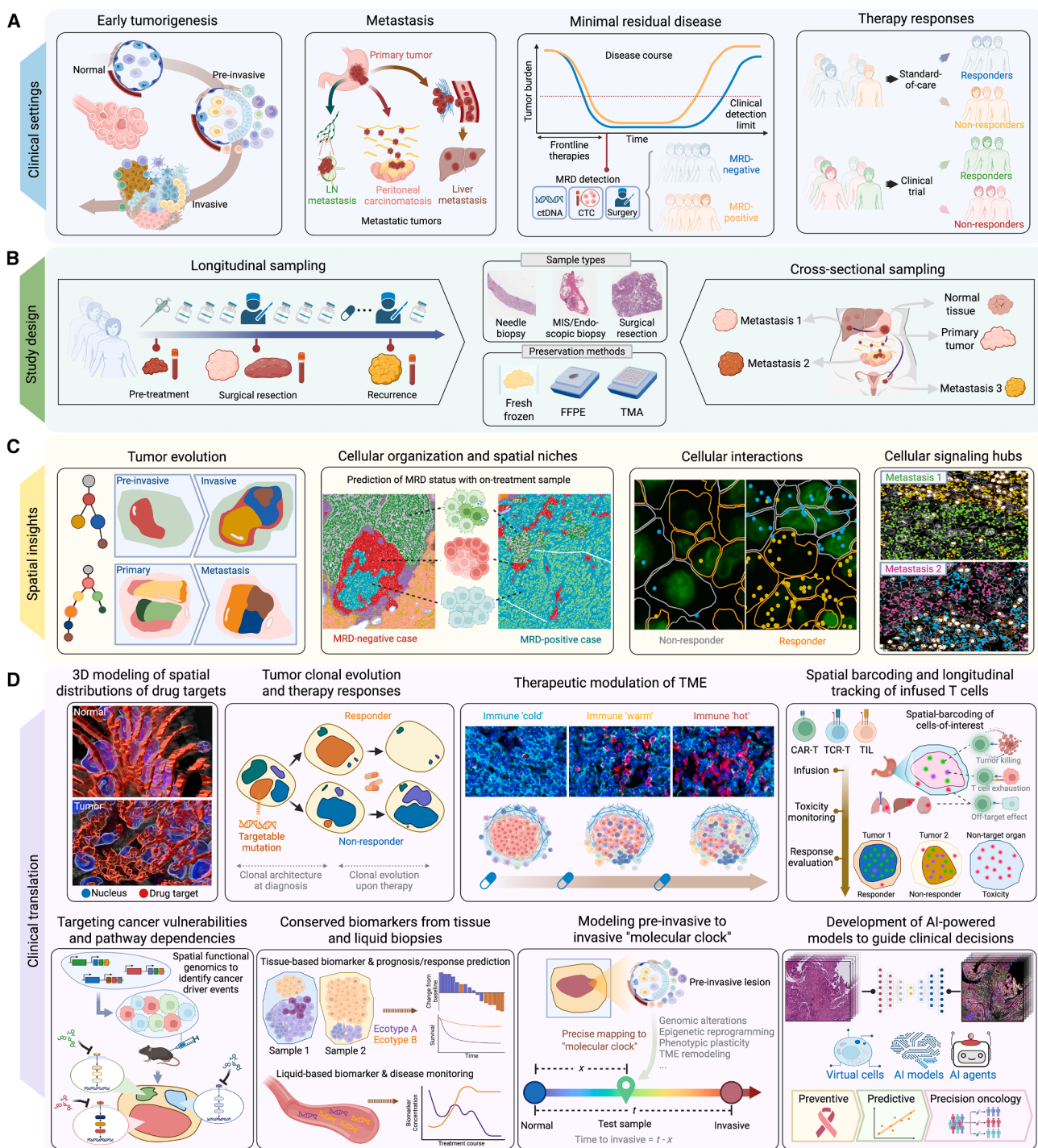


Figure 5. From spatial insights to clinical impact

- (A) Representative clinical scenarios where spatial profiling addresses key translational questions.
- (B) Integrated clinical-translational study designs incorporating spatial assays. MIS, minimally invasive surgery.
- (C) Novel insights from spatial data analysis.
- (D) Translation path from discovery to deployment. Spatial maps of drug target distribution courtesy of Dr. Tae Hyun Hwang (Vanderbilt University), used with permission.

Preservation methods dictate profiling modality choices: fresh-frozen tissues support discovery-level whole-transcriptome/metabolome assays and neoantigen discovery. FFPE tissues, most commonly available in retrospective cohorts, favor probe-based spatial transcriptomics and provide high quality histology. FFPE is compatible with most commercial spatial omics platforms, and probe sets targeting selected SNVs, as well as direct TCR/BCR sequencing, are now emerging. Pre-analytical variables (ischemia time, tissue fixation, section thickness) and co-collection strategies (paired FFPE/fresh-frozen, matched blood/plasma) should be protocolized. Thus, spatial platform choice should balance spatial resolution against capture area, FFPE compatibility, throughput, feasibility for multi-omics integration, and the primary scientific questions.

Clinical design determines data analysis framework: Cross-sectional sampling (such as primary and different metastatic tumors) allows for comparison of tumor heterogeneity across organ sites, while longitudinal sampling (such as pre- and post-treatment, or primary and recurrent tumors) enables temporal mapping of tumor and microenvironmental evolution with or without therapeutic pressure (Figures 5B–5D). The success of these analyses hinges on linking molecular features to tumor spatiotemporal dynamics and key clinical parameters. Careful alignment of study design, biospecimen logistics, and platform capabilities is essential to maximize clinical insights from cross-sectional or longitudinal spatial data.

Application in pre-cancer studies

Precancerous lesions arise within spatially organized tissue microenvironments and progress to invasive cancer, remain stable, or regress. Spatial omics enables high-resolution mapping of these lesions and their surrounding microenvironments over time, linking cellular, molecular, and architectural features to trajectories of progression or restraint (Figure 5). By charting these transitions *in situ*, we can identify risk markers and interception targets with direct translational relevance.

Spatial assays are beginning to pinpoint early molecular programs associated with malignant transition. For example, spatial profiling of serous tubal intraepithelial carcinomas, precursors to high-grade serous ovarian cancer, revealed upregulated interferon-response programs accompanied by an immunosuppressive milieu conducive to outgrowth.²¹⁶ In gastric intestinal metaplasia, spatial analyses identified a subset dominated by intestinal stem-cell lineages with transcriptomic convergence toward gastric cancer, supporting a putative lineage link.²¹⁷ Beyond intrinsic changes in epithelial states, multiple spatial studies highlight early tumor-TME crosstalk within discrete niches and dynamic remodeling during the premalignant-to-malignant transition, including the disruption of the tumor-stroma interface, macrophage polarization toward immunosuppressive states, and coordinated shifts in innate and adaptive immunity.^{218–222}

Consortia efforts, such as the HTAN Pre-Cancer Atlas Research Centers, are standardizing longitudinal, multi-modal spatial profiling across gastric, pancreatic, skin, low-grade glioma, and myeloma precursors to build comprehensive spatial atlases of pre-malignant states.²²³ These efforts will yield valuable insights into pre-cancer biology and pave the way for novel strategies in early detection and interception. Coupled with advanced machine

learning models, these atlases may enable “molecular clock” progression prediction frameworks (Figure 5D) that integrate spatial context to (i) precisely position each pre-invasive lesion along data-driven developmental trajectories, (ii) estimate the risk and timing of progression, i.e., predict whether and when a pre-invasive lesion will become invasive, and (iii) define actionable “interception windows” when intervention is most likely to succeed.

Spatial topography of multi-site metastasis

Metastasis is a multistep cascade—dissemination, seeding, and organ-specific outgrowth—shaped by tumor-stroma crosstalk (Figure 5). Spatial omics now resolves these events *in situ* across primary and metastatic sites, linking clonal evolution with cancer cell states, immune phenotypes, and tissue architecture.¹³⁰ By integrating spatial transcriptomics/proteomics with histopathology and, when available, DNA lineage readouts, these approaches connect genotypes to phenotypes and reveal local “signaling hubs” where perivascular niches, endothelial barriers, reactive stroma, and immune aggregates jointly govern colonization fitness. In PDAC, multi-site spatial analyses reconstructed patient-specific clonal architectures and uncovered organ-dependent lineage state shifts aligned with distinct immune microenvironments.¹³⁰ For example, a TGF β 1⁺ myCAFs—basal-like cancer cell axis associated with plasma cell exclusion via the CXCL12–CXCR4 signaling suggests site-agnostic rules whereby TME programs align with aggressive states during metastatic adaptation.¹³⁰ Spatial profiling in other contexts revealed that certain TME subsets may play a role in metastatic colonization, such as in brain metastasis, CLDN5-low endothelial cells demarcate permissive vascular niches linked to extravasation and outgrowth.²²⁴ Across tumor types, recurrent immunosuppressive architectures, often TAM-rich or CAF-dense, represent a hallmark of established metastases.^{130,225–227} Together, these insights motivate site-aware, context-dependent interventions tailored to the dominant microenvironmental constraints at each metastatic site.

Understanding minimal residual disease and therapy resistance

MRD denotes residual tumor that persists after frontline therapy but remains below the detection limit of standard imaging and serum markers. Incorporating surgical biopsies for MRD assessment—most notably via second-look laparoscopy (SLL) in ovarian cancer²²⁸—enables pairing tissue profiling with spatial omics to complement ctDNA-based assays. While liquid biopsy can flag residual disease, it may miss lesion-positive cases and offers limited context about the anatomical reservoir of disease or its microenvironmental features. Spatial omics maps MRD *in situ*, resolving cellular composition, cancer cell states, niche organization, and immune phenotypes. Beyond enabling clinically actionable biomarkers that can be integrated with liquid biopsies to enhance sensitivity and specificity, spatial MRD profiling provides deep insight into MRD biology and can inform treatment strategies. In SLL-based cohorts, systematic intraperitoneal biopsies and lavage from patients in clinically complete remission have enabled spatial characterization of MRD lesions, revealing hypoxia programs, upregulation of ATP-binding cassette transporters, and immune exclusion as potential resistance mechanisms.²²⁹

Therapeutically, interrogating MRD tissue opens a window for maintenance/interception strategies when disease burden is lowest and enables the use of MRD as a surrogate endpoint in early trials (e.g., NCT05739981). Longitudinal sampling further allows tracking of clonal and microenvironmental remodeling under therapy. This SLL-guided MRD sampling framework is adaptable to other peritoneal malignancies (e.g., gastric, colorectal). For extra-peritoneal tumors, image-guided core biopsies (e.g., of brain or lung metastases) can provide analogous spatial readouts, though the definition of MRD should be tailored based on tumor-specific contexts.

Spatial insights on cancer biomarkers

Spatial profiling resolves intratumoral heterogeneity and tissue architecture, enabling the discovery of biomarkers that complement clinicopathologic factors for diagnosis, prognosis, and response prediction (Figure 5). In breast cancer, large-cohort spatial omics studies show that spatial architecture-based tumor subgroupings predict survival beyond traditional clinical subtypes.^{230–232} These findings argue for incorporating spatial features into risk models and developing pragmatic, clinically deployable proxies. Beyond ecosystem-level descriptors, the spatial organization of key immune subsets—such as stem-like/tumor-reactive CD8⁺ T cells, TLSs, intratumoral immune triads,²³³ and perivascular DC-T cell hubs—correlates with response to ICB across cancers.^{234–237} Collectively, these advances are reshaping how we think about biomarkers: clinically meaningful spatial biomarkers are often composite patterns, such as specific cell-cell proximities, niche architectures, or co-occurring cell states, rather than a single gene, protein, or cell type that is simply “high” or “low” in a spatial region. Together, these studies provide mechanistic insight and nominate cellular or molecular biomarkers with clear translational potential. Clinical deployment of these biomarkers will require standardized assays, reproducible scoring thresholds, and harmonized interpretation.

Advanced computational frameworks, including foundation models, virtual cell simulators, and AI agents, trained on well-curated large-scale spatial multi-omics, histopathology, and clinical datasets, are poised to improve the prediction of therapeutic efficacy and toxicity and to generalize across platforms, accelerating decision support (Figure 5D). In parallel, liquid biopsy readouts (e.g., cell-free DNA) capable of inferring tissue spatial cellular architecture could enable noninvasive, real-time monitoring of tumor evolution and treatment response, complementing tissue-based assays that are susceptible to sampling bias and geographic heterogeneity.

Target discovery guided by spatial functional genomics

Spatial profiling empowers target discovery by linking tumor genetic alterations to phenotypes *in situ* within the architecture of clonal mosaics, stromal programs, and cell-cell circuits. By mapping tumor subclones alongside the TME, these assays reveal genotype-phenotype relationships, pathway dependencies, and interaction hubs that can be pharmacologically exploited. Perturb-map²³⁸ and Perturb-FISH²³⁹ provide spatial readouts of pooled genetic perturbations, showing how specific edits rewire local spatial architecture and cellular interactions. For instance, Dhainaut et al.²³⁸ showed that loss of *Tgfb2* in tumor cells drives immune exclusion in lung adenocarcinoma, nomi-

nating TGF- β axis modulation as a strategy to enhance immunotherapy efficacy. More broadly, high-throughput perturbation screens paired with spatial omics deliver multidimensional views of driver events and their microenvironmental consequences, informing the design of mechanism-anchored trials (Figure 5D).

Base-specific *in situ* sequencing (BaSISS) offers a complementary route by mapping genetically defined clones directly in tissues.¹⁰ In breast cancer, BaSISS revealed clone-specific niches and targets; for example, *HER2*-amplified clones residing in hypoxic regions with the concordant activation of oncogenic and hypoxia pathways¹⁰ highlighted the potential for rational, context-aware combinations. Integrating these technologies into prospective clinical studies with standardized sampling and longitudinal timepoints will elucidate how tumor evolutionary trajectories shape responses to standard-of-care (SOC) or investigational therapies, revealing clone- and niche-specific vulnerabilities for next-generation combinations.

CONCLUSIONS AND FUTURE DIRECTIONS

To bridge the gap between the translational promise outlined above and widespread clinical implementation, the field must now pivot from proof-of-concept discovery to rigorous standardization. While current high-plex workflows face hurdles in cost and throughput, short-term priorities should focus on validating candidate biomarkers and therapeutic targets identified through spatial assays, facilitating their translation into innovative clinical trials. In the longer term, technological development must shift toward cost-effective, high-throughput platforms that are compatible with routine sample processing and preservation procedures. Ultimately, achieving seamless integration of spatial profiling into routine pathology workflows will accelerate scientific discoveries and democratize access to these precision oncology tools.

Concurrently, next-generation technological advancements are propelling spatial omics to new frontiers. Emerging spatial perturbation platforms now enable functional genomics within the tissue context, leading to the identification of novel cancer driver events and pathway dependencies. Furthermore, spatial TCR and neoantigen profiling are facilitating the design of effective tumor vaccines; spatial barcoding technologies allow for the precise clonal tracking of infused T cells to decode response and toxicity in CAR-T cell therapies; live-system spatial imaging captures dynamic TME behavior; and 3D/4D multi-omics approaches are moving the field beyond static 2D slices, enabling the holistic visualization of cellular organization and molecular distribution within complex tissue architectures.

Machine learning (ML) is playing an increasingly important role in spatial research. AI models trained on histological or multimodal spatial datasets, such as virtual cells and AI agents, exhibit the potential to model complex cellular behaviors in the tissue context, identify distinct tumor ecotypes and spatial structures, and aid cancer diagnosis and risk stratification. Deep learning frameworks are also being used to decode ligand-receptor interaction networks and identify therapeutic targets. Predictive classifiers based on histological features or molecular signatures are undergoing clinical validation to inform therapeutic decisions. Most recently, the emerging field of pathomics – defined as the systemic extraction and analysis of quantitative features from histological images – has gained increasing

attention, supported by promising data from clinical cohorts.^{240,241} Integrating pathomics with spatial omics represents a powerful strategy for cancer biomarker discovery. Nonetheless, there are several remaining challenges regarding model interpretability, reproducibility, and seamless integration into clinical workflows. Moving forward, the development of scalable, transparent, and clinically interpretable AI frameworks will be critical for the successful translation of findings from spatial omics into personalized cancer care.

Advancing spatial omics will require sustained interdisciplinary collaboration. Clinicians, pathologists, computational scientists, and AI researchers must work in concert to develop tools, interpret complex datasets, and identify clinically meaningful findings. Cross-institutional initiatives such as HuBMAP and HTAN are instrumental in generating large-scale, high-quality datasets as shared resources for the broad scientific community. Effective collaboration is also fundamental for addressing key scientific challenges. For instance, a growing focus on TME dynamics - particularly how cellular ecosystems evolve during tumor progression and under therapeutic pressure - has emerged as a central theme in initiatives such as the Cancer Grand Challenges. In parallel with these collaborative efforts, ethical frameworks must be established to ensure transparency, equity, and accessibility, especially as spatial profiling becomes increasingly integrated into clinical research. The rapidly growing field of spatial omics offers a transformative lens through which to explore the complex spatial topography of tumors in unprecedented detail. By overcoming technical and computational barriers and fostering collaborations, the field is poised to generate profound insights that will transform clinical diagnostics and precision therapies, ultimately redefining precision oncology in the spatial era.

ACKNOWLEDGMENTS

This work was supported in part by the National Cancer Institute (U01CA294518, U01CA264583, R01CA266280) and Break Through Cancer. L.W. also acknowledges research support from the James P. Allison Institute and the Institute for Data Science in Oncology at The University of Texas MD Anderson Cancer Center. Figures were created with [BioRender.com](#).

AUTHOR CONTRIBUTIONS

All authors discussed the content of the article and contributed to writing, editing, and reviewing the article. Y.L. and Y.D. contributed equally. L.W. supervised the work.

DECLARATION OF INTERESTS

L.W. serves as a member of the Scientific Advisory Board for SELLAS Life Sciences and receives compensation outside the scope of this submitted work. All other authors declare no competing interest.

REFERENCES

1. Baysoy, A., Bai, Z., Satija, R., and Fan, R. (2023). The technological landscape and applications of single-cell multi-omics. *Nat. Rev. Mol. Cell Biol.* 24, 695–713. <https://doi.org/10.1038/s41580-023-00615-w>.
2. Tirosh, I., and Suva, M.L. (2024). Cancer cell states: Lessons from ten years of single-cell RNA-sequencing of human tumors. *Cancer Cell* 42, 1497–1506. <https://doi.org/10.1016/j.ccr.2024.08.005>.
3. Chen, J., Larsson, L., Swarbrick, A., and Lundeberg, J. (2024). Spatial landscapes of cancers: insights and opportunities. *Nat. Rev. Clin. Oncol.* 21, 660–674. <https://doi.org/10.1038/s41571-024-00926-7>.
4. Lewis, S.M., Asselin-Labat, M.L., Nguyen, Q., Berthelet, J., Tan, X., Wimmer, V.C., Merino, D., Rogers, K.L., and Naik, S.H. (2021). Spatial omics and multiplexed imaging to explore cancer biology. *Nat. Methods* 18, 997–1012. <https://doi.org/10.1038/s41592-021-01203-6>.
5. Cao, J., Li, C., Cui, Z., Deng, S., Lei, T., Liu, W., Yang, H., and Chen, P. (2024). Spatial Transcriptomics: A Powerful Tool in Disease Understanding and Drug Discovery. *Theranostics* 14, 2946–2968. <https://doi.org/10.7150/thno.95908>.
6. Park, H.E., Jo, S.H., Lee, R.H., Macks, C.P., Ku, T., Park, J., Lee, C.W., Hur, J.K., and Sohn, C.H. (2023). Spatial Transcriptomics: Technical Aspects of Recent Developments and Their Applications in Neuroscience and Cancer Research. *Adv. Sci.* 10, e2206939. <https://doi.org/10.1002/advs.202206939>.
7. Wang, Q., Zhi, Y., Zi, M., Mo, Y., Wang, Y., Liao, Q., Zhang, S., Gong, Z., Wang, F., Zeng, Z., et al. (2023). Spatially Resolved Transcriptomics Technology Facilitates Cancer Research. *Adv. Sci.* 10, e2302558. <https://doi.org/10.1002/advs.202302558>.
8. Gong, D., Arbesfeld-Qiu, J.M., Perrault, E., Bae, J.W., and Hwang, W.L. (2024). Spatial oncology: Translating contextual biology to the clinic. *Cancer Cell* 42, 1653–1675. <https://doi.org/10.1016/j.ccr.2024.09.001>.
9. Galeano Niño, J.L., Wu, H., LaCourse, K.D., Kempchinsky, A.G., Barriales, A., Barber, B., Futran, N., Houlton, J., Sather, C., Sicinska, E., et al. (2022). Effect of the intratumoral microbiota on spatial and cellular heterogeneity in cancer. *Nature* 611, 810–817. <https://doi.org/10.1038/s41586-022-05435-0>.
10. Lomakin, A., Svedlund, J., Strell, C., Gataric, M., Shmatko, A., Rukhovich, G., Park, J.S., Ju, Y.S., Dentro, S., Kleshchevnikov, V., et al. (2022). Spatial genomics maps the structure, nature and evolution of cancer clones. *Nature* 611, 594–602. <https://doi.org/10.1038/s41586-022-05425-2>.
11. Moses, L., and Pachter, L. (2022). Museum of spatial transcriptomics. *Nat. Methods* 19, 534–546. <https://doi.org/10.1038/s41592-022-01409-2>.
12. Du, J., Yang, Y.C., An, Z.J., Zhang, M.H., Fu, X.H., Huang, Z.F., Yuan, Y., and Hou, J. (2023). Advances in spatial transcriptomics and related data analysis strategies. *J. Transl. Med.* 21, 330. <https://doi.org/10.1186/s12967-023-04150-2>.
13. (2024). Method of the Year 2024: spatial proteomics. *Nat. Methods* 21, 2195–2196. <https://doi.org/10.1038/s41592-024-02565-3>.
14. Liu, Y., Sinjab, A., Min, J., Han, G., Paradiso, F., Zhang, Y., Wang, R., Pei, G., Dai, Y., Liu, Y., et al. (2025). Conserved spatial subtypes and cellular neighborhoods of cancer-associated fibroblasts revealed by single-cell spatial multi-omics. *Cancer Cell* 43, 905–924.e6. <https://doi.org/10.1016/j.ccr.2025.03.004>.
15. Bassiouni, R., Gibbs, L.D., Craig, D.W., Carpten, J.D., and McEachron, T.A. (2021). Applicability of spatial transcriptional profiling to cancer research. *Mol. Cell* 81, 1631–1639. <https://doi.org/10.1016/j.molcel.2021.03.016>.
16. Elhanani, O., Ben-Uri, R., and Keren, L. (2023). Spatial profiling technologies illuminate the tumor microenvironment. *Cancer Cell* 41, 404–420. <https://doi.org/10.1016/j.ccr.2023.01.010>.
17. Liu, L., Chen, A., Li, Y., Mulder, J., Heyn, H., and Xu, X. (2024). Spatiotemporal omics for biology and medicine. *Cell* 187, 4488–4519. <https://doi.org/10.1016/j.cell.2024.07.040>.
18. Jin, Y., Zuo, Y., Li, G., Liu, W., Pan, Y., Fan, T., Fu, X., Yao, X., and Peng, Y. (2024). Advances in spatial transcriptomics and its applications in cancer research. *Mol. Cancer* 23, 129. <https://doi.org/10.1186/s12943-024-02040-9>.
19. Moffitt, J.R., Lundberg, E., and Heyn, H. (2022). The emerging landscape of spatial profiling technologies. *Nat. Rev. Genet.* 23, 741–759. <https://doi.org/10.1038/s41576-022-00515-3>.
20. Tian, L., Chen, F., and Macosko, E.Z. (2023). The expanding vistas of spatial transcriptomics. *Nat. Biotechnol.* 41, 773–782. <https://doi.org/10.1038/s41587-022-01448-2>.

21. Lubeck, E., Coskun, A.F., Zhiyentayev, T., Ahmad, M., and Cai, L. (2014). Single-cell *in situ* RNA profiling by sequential hybridization. *Nat. Methods* 11, 360–361. <https://doi.org/10.1038/nmeth.2892>.
22. Korenberg, J.R., Yang-Feng, T., Schreck, R., and Chen, X.N. (1992). Using fluorescence *in situ* hybridization (FISH) in genome mapping. *Trends Biotechnol.* 10, 27–32.
23. T, R.G., and Stollar, B.D. (1977). High resolution detection of DNA-RNA hybrids *in situ* by indirect immunofluorescence. *Nature* 265, 472–473. <https://doi.org/10.1038/265472a0>.
24. Femino, A.M., Fay, F.S., Fogarty, K., and Singer, R.H. (1998). Visualization of single RNA transcripts *in situ*. *Science* 280, 585–590. <https://doi.org/10.1126/science.280.5363.585>.
25. Raj, A., van den Bogaard, P., Rifkin, S.A., van Oudenaarden, A., and Tyagi, S. (2008). Imaging individual mRNA molecules using multiple singly labeled probes. *Nat. Methods* 5, 877–879. <https://doi.org/10.1038/nmeth.1253>.
26. He, S., Bhatt, R., Brown, C., Brown, E.A., Buhr, D.L., Chantranuvatana, K., Danaher, P., Dunaway, D., Garrison, R.G., Geiss, G., et al. (2022). High-plex imaging of RNA and proteins at subcellular resolution in fixed tissue by spatial molecular imaging. *Nat. Biotechnol.* 40, 1794–1806. <https://doi.org/10.1038/s41587-022-01483-z>.
27. Janesick, A., Shelansky, R., Gottscho, A.D., Wagner, F., Williams, S.R., Rouault, M., Beliakoff, G., Morrison, C.A., Oliveira, M.F., Sicherman, J.T., et al. (2023). High resolution mapping of the tumor microenvironment using integrated single-cell, spatial and *in situ* analysis. *Nat. Commun.* 14, 8353. <https://doi.org/10.1038/s41467-023-43458-x>.
28. Wang, G., Moffitt, J.R., and Zhuang, X. (2018). Multiplexed imaging of high-density libraries of RNAs with MERFISH and expansion microscopy. *Sci. Rep.* 8, 4847. <https://doi.org/10.1038/s41598-018-22297-7>.
29. Lee, J.H., Daugharty, E.R., Scheiman, J., Kalhor, R., Ferrante, T.C., Terry, R., Turczyk, B.M., Yang, J.L., Lee, H.S., Aach, J., et al. (2015). Fluorescent *in situ* sequencing (FISSEQ) of RNA for gene expression profiling in intact cells and tissues. *Nat. Protoc.* 10, 442–458. <https://doi.org/10.1038/nprot.2014.191>.
30. Wang, X., Allen, W.E., Wright, M.A., Sylwestrak, E.L., Samusik, N., Vesuna, S., Evans, K., Liu, C., Ramakrishnan, C., Liu, J., et al. (2018). Three-dimensional intact-tissue sequencing of single-cell transcriptional states. *Science* 361, eaat5691. <https://doi.org/10.1126/science.aat5691>.
31. Eng, C.H.L., Lawson, M., Zhu, Q., Dries, R., Koulena, N., Takei, Y., Yun, J., Cronin, C., Karp, C., Yuan, G.C., and Cai, L. (2019). Transcriptome-scale super-resolved imaging in tissues by RNA seqFISH. *Nature* 568, 235–239. <https://doi.org/10.1038/s41586-019-1049-y>.
32. Alon, S., Goodwin, D.R., Sinha, A., Wassie, A.T., Chen, F., Daugharty, E.R., Bando, Y., Kajita, A., Xue, A.G., Marrett, K., et al. (2021). Expansion sequencing: Spatially precise *in situ* transcriptomics in intact biological systems. *Science* 371, eaax2656. <https://doi.org/10.1126/science.aax2656>.
33. Hu, K.H., Eichorst, J.P., McGinnis, C.S., Patterson, D.M., Chow, E.D., Kersten, K., Jameson, S.C., Gartner, Z.J., Rao, A.A., and Krummel, M.F. (2020). ZipSeq: barcoding for real-time mapping of single cell transcriptomes. *Nat. Methods* 17, 833–843. <https://doi.org/10.1038/s41592-020-0880-2>.
34. Lee, Y., Bogdanoff, D., Wang, Y., Hartoularos, G.C., Woo, J.M., Mowery, C.T., Nisonoff, H.M., Lee, D.S., Sun, Y., Lee, J., et al. (2021). XYZeq: Spatially resolved single-cell RNA sequencing reveals expression heterogeneity in the tumor microenvironment. *LID* - 10.1126/sciad-v.abg4755 [doi] LID - abg4755. *Sci. Adv.* 7, abg4755. <https://doi.org/10.1126/sciadv.abg4755>.
35. Srivatsan, S.R., Regier, M.C., Barkan, E., Franks, J.M., Packer, J.S., Grosjean, P., Duran, M., Saxton, S., Ladd, J.J., Spielmann, M., et al. (2021). Embryo-scale, single-cell spatial transcriptomics. *Science* 373, 111–117. <https://doi.org/10.1126/science.abb9536>.
36. Russell, A.J.C., Weir, J.A., Nadaf, N.M., Shabot, M., Kumar, V., Kambhampati, S., Raichur, R., Marrero, G.J., Liu, S., Balderrama, K.S., et al. (2024). Slide-tags enables single-nucleus barcoding for multimodal spatial genomics. *Nature* 625, 101–109. <https://doi.org/10.1038/s41586-023-06837-4>.
37. Stickels, R.R., Murray, E., Kumar, P., Li, J., Marshall, J.L., Di Bella, D.J., Arlotta, P., Macosko, E.Z., and Chen, F. (2021). Highly sensitive spatial transcriptomics at near-cellular resolution with Slide-seqV2. *Nat. Biotechnol.* 39, 313–319. <https://doi.org/10.1038/s41587-020-0739-1>.
38. Rodrigues, S.G., Stickels, R.R., Goeva, A., Martin, C.A., Murray, E., Vandenburg, C.R., Welch, J., Chen, L.M., Chen, F., and Macosko, E.Z. (2019). Slide-seq: A scalable technology for measuring genome-wide expression at high spatial resolution. *Science* 363, 1463–1467. <https://doi.org/10.1126/science.aaw1219>.
39. Vickovic, S., Eraslan, G., Salmén, F., Klughammer, J., Stenbeck, L., Schapiro, D., Äijö, T., Bonneau, R., Bergenstråhlé, L., Navarro, J.F., et al. (2019). High-definition spatial transcriptomics for *in situ* tissue profiling. *Nat. Methods* 16, 987–990. <https://doi.org/10.1038/s41592-019-0548-y>.
40. Liu, Y., Yang, M., Deng, Y., Su, G., Enninful, A., Guo, C.C., Tebaldi, T., Zhang, D., Kim, D., Bai, Z., et al. (2020). High-Spatial-Resolution Multi-Omics Sequencing via Deterministic Barcoding in Tissue. *Cell* 183, 1665–1681.e18. <https://doi.org/10.1016/j.cell.2020.10.026>.
41. Kim, Y., Cheng, W., Cho, C.S., Hwang, Y., Si, Y., Park, A., Schrank, M., Hsu, J.E., Anacleto, A., Xi, J., et al. (2025). Seq-Scope: repurposing Illumina sequencing flow cells for high-resolution spatial transcriptomics. *Nat. Protoc.* 20, 643–689. <https://doi.org/10.1038/s41596-024-01065-0>.
42. Chen, A., Liao, S., Cheng, M., Ma, K., Wu, L., Lai, Y., Qiu, X., Yang, J., Xu, J., Hao, S., et al. (2022). Spatiotemporal transcriptomic atlas of mouse organogenesis using DNA nanoball-patterned arrays. *Cell* 185, 1777–1792.e21.
43. Fu, X., Sun, L., Dong, R., Chen, J.Y., Silakit, R., Condon, L.F., Lin, Y., Lin, S., Palmiter, R.D., and Gu, L. (2022). Polony gels enable amplifiable DNA stamping and spatial transcriptomics of chronic pain. *Cell* 185, 4621–4633.e17. <https://doi.org/10.1016/j.cell.2022.10.021>.
44. Marx, V. (2021). Method of the Year: spatially resolved transcriptomics. *Nat. Methods* 18, 9–14. <https://doi.org/10.1038/s41592-020-01033-y>.
45. Crosetto, N., Bienko, M., and van Oudenaarden, A. (2015). Spatially resolved transcriptomics and beyond. *Nat. Rev. Genet.* 16, 57–66. <https://doi.org/10.1038/nrg3832>.
46. Schürch, C.M., Bhate, S.S., Barlow, G.L., Phillips, D.J., Noti, L., Zlobec, I., Chu, P., Black, S., Demeter, J., McIlwain, D.R., et al. (2020). Coordinated cellular neighborhoods orchestrate antitumoral immunity at the colorectal cancer invasive front. *Cell* 182, 1341–1359. <https://doi.org/10.1016/j.cell.2020.07.005>.
47. Milosevic, V. (2023). Different approaches to Imaging Mass Cytometry data analysis. *Bioinform. Adv.* 3, vbad046. <https://doi.org/10.1093/bio-adv/vbad046>.
48. Aichler, M., and Walch, A. (2015). MALDI Imaging mass spectrometry: current frontiers and perspectives in pathology research and practice. *Lab. Invest.* 95, 422–431. <https://doi.org/10.1038/labinvest.2014.156>.
49. Claude, E., Jones, E.A., and Pringle, S.D. (2017). DESI Mass Spectrometry Imaging (MSI). *Methods Mol. Biol.* 1618, 65–75. https://doi.org/10.1007/978-1-4939-7051-3_7.
50. Lockyer, N.P., Aoyagi, S., Fletcher, J.S., Gilmore, I.S., van der Heide, P.A.W., Moore, K.L., Tyler, B.J., and Weng, L.-T. (2024). Secondary ion mass spectrometry. *Nat. Rev. Methods Primers* 4, 32. <https://doi.org/10.1038/s43586-024-00311-9>.
51. Spangenberg, P., Bessler, S., Widera, L., Bottek, J., Richter, M., Thiebes, S., Siemes, D., Krauß, S.D., Migas, L.G., Kasarla, S.S., et al. (2025). msiFlow: automated workflows for reproducible and scalable multimodal mass spectrometry imaging and microscopy data analysis. *Nat. Commun.* 16, 1065. <https://doi.org/10.1038/s41467-024-55306-7>.
52. Vicari, M., Mirzaezaheh, R., Nilsson, A., Shariatgorji, R., Bjärnerot, P., Larsson, L., Lee, H., Nilsson, M., Foyer, J., Ekval, M., et al. (2024). Spatial multimodal analysis of transcriptomes and metabolomes in tissues. *Nat. Biotechnol.* 42, 1046–1050. <https://doi.org/10.1038/s41587-023-01937-y>.

53. Takei, Y., Yang, Y., White, J., Goronzy, I.N., Yun, J., Prasad, M., Ombrelli, L.J., Schindler, S., Bhat, P., Guttman, M., and Cai, L. (2025). Spatial multi-omics reveals cell-type-specific nuclear compartments. *Nature* 641, 1037–1047. <https://doi.org/10.1038/s41586-025-08838-x>.
54. Mo, C.K., Liu, J., Chen, S., Storrs, E., Targino da Costa, A.L.N., Houston, A., Wendl, M.C., Jayasinghe, R.G., Iglesia, M.D., Ma, C., et al. (2024). Tumour evolution and microenvironment interactions in 2D and 3D space. *Nature* 634, 1178–1186. <https://doi.org/10.1038/s41586-024-08087-4>.
55. Braxton, A.M., Kiemen, A.L., Grahn, M.P., Forjaz, A., Parksong, J., Mahesh Babu, J., Lai, J., Zheng, L., Niknafs, N., Jiang, L., et al. (2024). 3D genomic mapping reveals multifocality of human pancreatic precancers. *Nature* 629, 679–687. <https://doi.org/10.1038/s41586-024-07359-3>.
56. Lin, J.R., Wang, S., Coy, S., Chen, Y.A., Yapp, C., Tyler, M., Nariya, M.K., Heiser, C.N., Lau, K.S., Santagata, S., and Sorger, P.K. (2023). Multiplexed 3D atlas of state transitions and immune interaction in colorectal cancer. *Cell* 186, 363–381.e19. <https://doi.org/10.1016/j.cell.2022.12.028>.
57. Liu, Y., DiStasio, M., Su, G., Asashima, H., Enninfu, A., Qin, X., Deng, Y., Nam, J., Gao, F., Bordignon, P., et al. (2023). High-plex protein and whole transcriptome co-mapping at cellular resolution with spatial CITE-seq. *Nat. Biotechnol.* 41, 1405–1409. <https://doi.org/10.1038/s41587-023-01676-0>.
58. Bai, Z., Zhang, D., Gao, Y., Tao, B., Zhang, D., Bao, S., Enninfu, A., Wang, Y., Li, H., Su, G., et al. (2024). Spatially exploring RNA biology in archival formalin-fixed paraffin-embedded tissues. *Cell* 187, 6760–6779.e24. <https://doi.org/10.1016/j.cell.2024.09.001>.
59. Wang, L., Li, M., and Hwang, T.H. (2024). The 3D Revolution in Cancer Discovery. *Cancer Discov.* 14, 625–629. <https://doi.org/10.1158/2159-8290.CD-23-1499>.
60. Mo, C.K., Liu, J., Chen, S., Storrs, E., Targino da Costa, A.L.N., Houston, A., Wendl, M.C., Jayasinghe, R.G., Iglesia, M.D., Ma, C., et al. (2024). Tumour evolution and microenvironment interactions in 2D and 3D space. *Nature* 634, 1178–1186. <https://doi.org/10.1038/s41586-024-08087-4>.
61. Ferri-Borgogno, S., Burks, J.K., Seeley, E.H., McKee, T.D., Stolley, D.L., Basi, A.V., Gomez, J.A., Gamal, B.T., Ayyadhyury, S., Lawson, B.C., et al. (2024). Molecular, Metabolic, and Subcellular Mapping of the Tumor Immune Microenvironment via 3D Targeted and Non-Targeted Multiplex Multi-Omics Analyses. *Cancers (Basel)* 16, 846. <https://doi.org/10.3390/cancers16050846>.
62. Park, J., Shin, S.J., Kim, G., Cho, H., Ryu, D., Ahn, D., Heo, J.E., Clemenceau, J.R., Barnfather, I., Kim, M., et al. (2025). Revealing 3D microanatomical structures of unlabeled thick cancer tissues using holotomography and virtual H&E staining. *Nat. Commun.* 16, 4781. <https://doi.org/10.1038/s41467-025-59820-0>.
63. Glaser, A.K., Reder, N.P., Chen, Y., McCarty, E.F., Yin, C., Wei, L., Wang, Y., True, L.D., and Liu, J.T.C. (2017). Light-sheet microscopy for slide-free non-destructive pathology of large clinical specimens. *Nat. Biomed. Eng.* 1, 0084. <https://doi.org/10.1038/s41551-017-0084>.
64. Yapp, C., Nirmal, A.J., Zhou, F., Wong, A.Y.H., Tefft, J.B., Lu, Y.D., Shang, Z., Maliga, Z., Llopis, P.M., Murphy, G.F., et al. (2025). Highly multiplexed 3D profiling of cell states and immune niches in human tumors. *Nat. Methods* 22, 2180–2193. <https://doi.org/10.1038/s41592-025-02824-x>.
65. Liu, J.T.C., Glaser, A.K., Bera, K., True, L.D., Reder, N.P., Eliceiri, K.W., and Madabhushi, A. (2021). Harnessing non-destructive 3D pathology. *Nat. Biomed. Eng.* 5, 203–218. <https://doi.org/10.1038/s41551-020-00681-x>.
66. Glaser, A.K., Bishop, K.W., Barner, L.A., Susaki, E.A., Kubota, S.I., Gao, G., Serafin, R.B., Balaram, P., Turschak, E., Nicovich, P.R., et al. (2022). A hybrid open-top light-sheet microscope for versatile multi-scale imaging of cleared tissues. *Nat. Methods* 19, 613–619. <https://doi.org/10.1038/s41592-022-01468-5>.
67. Song, A.H., Williams, M., Williamson, D.F.K., Chow, S.S.L., Jaume, G., Gao, G., Zhang, A., Chen, B., Baras, A.S., Serafin, R., et al. (2024). Analysis of 3D pathology samples using weakly supervised AI. *Cell* 187, 2502–2520.e17. <https://doi.org/10.1016/j.cell.2024.03.035>.
68. Kim, G., Hugonnet, H., Kim, K., Lee, J.-H., Lee, S.S., Ha, J., Lee, C., Park, H., Yoon, K.-J., Shin, Y., et al. (2024). Holotomography. *Nat. Rev. Methods Primers* 4, 51. <https://doi.org/10.1038/s43586-024-00327-1>.
69. Lee, M.J., Lee, J., Ha, J., Kim, G., Kim, H.J., Lee, S., Koo, B.K., and Park, Y. (2024). Long-term three-dimensional high-resolution imaging of live unlabeled small intestinal organoids via low-coherence holotomography. *Exp. Mol. Med.* 56, 2162–2170. <https://doi.org/10.1038/s12276-024-01312-0>.
70. Weigert, M., and Schmidt, U. (2022). Nuclei Instance Segmentation and Classification in Histopathology Images with Stardist. In 2022 IEEE International Symposium on Biomedical Imaging Challenges (ISBIC).
71. Heidari, E., Moorman, A., Unyi, D., Pasnuri, N., Rukhovich, G., Calafato, D., Mathioudaki, A., Chan, J.M., Nawy, T., Gerstung, M., et al. (2025). Segger: Fast and Accurate Cell Segmentation of Imaging-Based Spatial Transcriptomics Data (Cold Spring Harbor Laboratory).
72. Ni, Z., Prasad, A., Chen, S., Halberg, R.B., Arkin, L.M., Drolet, B.A., Newton, M.A., and Kendziora, C. (2022). SpotClean adjusts for spot swapping in spatial transcriptomics data. *Nat. Commun.* 13, 2971. <https://doi.org/10.1038/s41467-022-30587-y>.
73. Zhang, H., Hunter, M.V., Chou, J., Quinn, J.F., Zhou, M., White, R.M., and Tansey, W. (2023). BayesTME: An end-to-end method for multiscale spatial transcriptional profiling of the tissue microenvironment. *Cell Syst.* 14, 605–619.e7. <https://doi.org/10.1016/j.cels.2023.06.003>.
74. Bilous, M., Buszta, D., Bac, J., Kang, S., Dong, Y., Tissot, S., Andre, S., Alexandre-Gaveta, M., Voize, C., Peters, S., et al. (2025). From Transcripts to Cells: Dissecting Sensitivity, Signal Contamination, and Specificity in Xenium Spatial Transcriptomics (Cold Spring Harbor Laboratory).
75. Salim, A., Bhuvu, D.D., Chen, C., Tan, C.W., Yang, P., Davis, M.J., and Yang, J.Y.H. (2025). SpaNorm: spatially-aware normalization for spatial transcriptomics data. *Genome Biol.* 26, 109. <https://doi.org/10.1186/s13059-025-03565-y>.
76. Shang, L., and Zhou, X. (2022). Spatially aware dimension reduction for spatial transcriptomics. *Nat. Commun.* 13, 7203. <https://doi.org/10.1038/s41467-022-34879-1>.
77. Hu, J.A.-O., Li, X., Coleman, K.A.-O., Schroeder, A., Ma, N.A.-O., Irwin, D.A.-O., Lee, E.A.-O., Shinohara, R.T., and Li, M.A.-O. (2021). SpaGCN: Integrating gene expression, spatial location and histology to identify spatial domains and spatially variable genes by graph convolutional network. *Nat. Methods* 18, 1342–1351. <https://doi.org/10.1038/s41592-021-01255-8>.
78. Hu, J., Coleman, K., Zhang, D., Lee, E.B., Kadara, H., Wang, L., and Li, M. (2023). Deciphering tumor ecosystems at super resolution from spatial transcriptomics with TESLA. *Cell Syst.* 14, 404–417.e4. <https://doi.org/10.1016/j.cels.2023.03.008>.
79. Zhang, D., Schroeder, A., Yan, H., Yang, H., Hu, J., Lee, M.Y.Y., Cho, K.S., Susztak, K., Xu, G.X., Feldman, M.D., et al. (2024). Inferring super-resolution tissue architecture by integrating spatial transcriptomics with histology. *Nat. Biotechnol.* 42, 1372–1377. <https://doi.org/10.1038/s41587-023-02019-9>.
80. Chen, R.J., Ding, T., Lu, M.Y., Williamson, D.F.K., Jaume, G., Song, A.H., Chen, B., Zhang, A., Shao, D., Shaban, M., et al. (2024). Towards a general-purpose foundation model for computational pathology. *Nat. Med.* 30, 850–862. <https://doi.org/10.1038/s41591-024-02857-3>.
81. Shaban, M., Chang, Y., Qiu, H., Yeo, Y.Y., Song, A.H., Jaume, G., Wang, Y., Weishaupt, L.L., Ding, T., Vaidya, A., et al. (2025). A Foundation Model for Spatial Proteomics. <https://doi.org/10.48550/arXiv.2506.03373>.
82. Polański, K., Bartolomé-Casado, R., Sarropoulos, I., Xu, C., England, N., Jahnsen, F.L., Teichmann, S.A., and Yayon, N. (2024). Bin2cell reconstructs cells from high resolution Visium HD data. *Bioinformatics* 40, btae546. <https://doi.org/10.1093/bioinformatics/btae546>.
83. Guo, J., Sarafinovska, S., Hagensen, R.A., Valentine, M.C., Dougherty, J.D., Mitra, R.D., and Muegge, B.D. (2025). SMURF Reconstructs Single-Cells from Visium HD Data to Reveal Zonation of Transcriptional Programs in the Intestine (Cold Spring Harbor Laboratory).

84. Shen, R., Liu, L., Wu, Z., Zhang, Y., Yuan, Z., Guo, J., Yang, F., Zhang, C., Chen, B., Feng, W., et al. (2022). Spatial-ID: a cell typing method for spatially resolved transcriptomics via transfer learning and spatial embedding. *Nat. Commun.* 13, 7640. <https://doi.org/10.1038/s41467-022-35288-0>.
85. Grisanti Canozo, F.J., Zuo, Z., Martin, J.F., and Samee, M.A.H. (2022). Cell-type modeling in spatial transcriptomics data elucidates spatially variable colocalization and communication between cell-types in mouse brain. *Cell Syst.* 13, 58–70.e5. <https://doi.org/10.1016/j.cels.2021.09.004>.
86. Singhal, V., Chou, N., Lee, J., Yue, Y., Liu, J., Chock, W.K., Lin, L., Chang, Y.C., Teo, E.M.L., Aow, J., et al. (2024). BANKSY unifies cell typing and tissue domain segmentation for scalable spatial omics data analysis. *Nat. Genet.* 56, 431–441. <https://doi.org/10.1038/s41588-024-01664-3>.
87. Cable, D.M., Murray, E., Zou, L.S., Goeva, A., Macosko, E.Z., Chen, F., and Irizarry, R.A. (2022). Robust decomposition of cell type mixtures in spatial transcriptomics. *Nat. Biotechnol.* 40, 517–526. <https://doi.org/10.1038/s41587-021-00830-w>.
88. Elosua-Bayes, M., Nieto, P., Mereu, E., Gut, I., and Heyn, H. (2021). SPOTlight: seeded NMF regression to deconvolute spatial transcriptomics spots with single-cell transcriptomes. *Nucleic Acids Res.* 49, e50. <https://doi.org/10.1093/nar/gkab043>.
89. Kleshchchevnikov, V., Shmatko, A., Dann, E., Aivazidis, A., King, H.W., Li, T., Elmentaita, R., Lomakin, A., Kedlian, V., Gayoso, A., et al. (2022). Cell2location maps fine-grained cell types in spatial transcriptomics. *Nat. Biotechnol.* 40, 661–671. <https://doi.org/10.1038/s41587-021-01139-4>.
90. Biancalani, T., Scalia, G., Buffoni, L., Avasthi, R., Lu, Z., Sanger, A., Tokcan, N., Vanderburg, C.R., Segerstolpe, Å., Zhang, M., et al. (2021). Deep learning and alignment of spatially resolved single-cell transcriptomes with Tangram. *Nat. Methods* 18, 1352–1362. <https://doi.org/10.1038/s41592-021-01264-7>.
91. Vahid, M.R., Brown, E.L., Steen, C.B., Zhang, W., Jeon, H.S., Kang, M., Gentles, A.J., and Newman, A.M. (2023). High-resolution alignment of single-cell and spatial transcriptomes with CytoSPACE. *Nat. Biotechnol.* 41, 1543–1548. <https://doi.org/10.1038/s41587-023-01697-9>.
92. Yang, J., Zheng, Z., Jiao, Y., Yu, K., Bhataria, S., Yang, X., Natarajan, S., Zhang, J., Pan, Q., Easton, J., et al. (2025). Spotiphy enables single-cell spatial whole transcriptomics across an entire section. *Nat. Methods* 22, 724–736. <https://doi.org/10.1038/s41592-025-02622-5>.
93. Nader, K., Tasci, M., Janevski, A., Erickson, A., Verschuren, E.W., Aittokallio, T., and Mihkinen, M. (2024). ScType enables fast and accurate cell type identification from spatial transcriptomics data. *Bioinformatics* 40, btae426. <https://doi.org/10.1093/bioinformatics/btae426>.
94. Geras, A., Darvish Shafiqi, S., Domżał, K., Filipiuk, I., Raczkowska, A., Szymczak, P., Toosi, H., Kaczmarek, L., Koperski, Ł., Lagergren, J., et al. (2023). Celloscope: a probabilistic model for marker-gene-driven cell type deconvolution in spatial transcriptomics data. *Genome Biol.* 24, 120. <https://doi.org/10.1186/s13059-023-02951-8>.
95. Benjamin, K., Bhandari, A., Kepple, J.D., Qi, R., Shang, Z., Xing, Y., An, Y., Zhang, N., Hou, Y., Crockford, T.L., et al. (2024). Multiscale topology classifies cells in subcellular spatial transcriptomics. *Nature* 630, 943–949. <https://doi.org/10.1038/s41586-024-07563-1>.
96. Aggarwal, B., and Sinha, S. (2025). CellSP: Module Discovery and Visualization for Subcellular Spatial Transcriptomics Data (Cold Spring Harbor Laboratory).
97. Mah, C.K., Ahmed, N., Lopez, N.A., Lam, D.C., Pong, A., Monell, A., Kern, C., Han, Y., Prasad, G., Cesnik, A.J., et al. (2024). Bento: a toolkit for subcellular analysis of spatial transcriptomics data. *Genome Biol.* 25, 82. <https://doi.org/10.1186/s13059-024-03217-7>.
98. Rajachandran, S., Xu, Q., Cao, Q., Zhang, X., Chen, F.A.-O., Mangiameli, S.M., and Chen, H.A.-O. (2024). Subcellular level spatial transcriptomics with PHOTON. Preprint at bioRxiv. <https://doi.org/10.1101/2024.09.10.612328>.
99. Efremova, M., Vento-Tormo, M., Teichmann, S.A., and Vento-Tormo, R. (2020). CellPhoneDB: inferring cell-cell communication from combined expression of multi-subunit ligand-receptor complexes. *Nat. Protoc.* 15, 1484–1506. <https://doi.org/10.1038/s41596-020-0292-x>.
100. Jin, S., Plikus, M.V., and Nie, Q. (2025). CellChat for systematic analysis of cell-cell communication from single-cell and spatially resolved transcriptomics. *Nat. Protoc.* 20, 180–219. <https://doi.org/10.1038/s41596-024-01045-4>.
101. Dries, R., Zhu, Q., Dong, R., Eng, C.-H.L., Li, H., Liu, K., Fu, Y., Zhao, T., Sarkar, A., Bao, F., et al. (2021). Giotto: a toolbox for integrative analysis and visualization of spatial expression data. *Genome Biol.* 22, 78. <https://doi.org/10.1186/s13059-021-02286-2>.
102. Wang, H., Li, J., Jing, S., Lin, P., Qiu, Y., Yan, X., Yuan, J., Tang, Z., Li, Y., Zhang, H., et al. (2025). SOAPy: a Python package to dissect spatial architecture, dynamics, and communication. *Genome Biol.* 26, 80. <https://doi.org/10.1186/s13059-025-03550-5>.
103. Palla, G., Spitzer, H., Klein, M., Fischer, D., Schaar, A.C., Kuemmerle, L.B., Rybakov, S., Ibarra, I.L., Holmberg, O., Virshup, I., et al. (2022). Squidpy: a scalable framework for spatial omics analysis. *Nat. Methods* 19, 171–178. <https://doi.org/10.1038/s41592-021-01358-2>.
104. Qiu, X., Zhu, D.Y., Yao, J., Jing, Z., Zuo, L., Wang, M., Min, K.H., Pan, H., Wang, S., Liao, S., et al. (2022). Spateo: Multidimensional Spatiotemporal Modeling of Single-Cell Spatial Transcriptomics (Cold Spring Harbor Laboratory).
105. Liu, J., Manabe, H., Qian, W., Wang, Y., Gu, Y., Yan Chu, A.K., Gad hví, G., Song, Y., Ono, N., and Welch, J.D. (2024). CytoSignal Detects Locations and Dynamics of Ligand-Receptor Signaling at Cellular Resolution from Spatial Transcriptomic Data (Cold Spring Harbor Laboratory).
106. Cang, Z., Zhao, Y., Almet, A.A., Stabell, A., Ramos, R., Plikus, M.V., Atwood, S.X., and Nie, Q. (2023). Screening cell-cell communication in spatial transcriptomics via collective optimal transport. *Nat. Methods* 20, 218–228. <https://doi.org/10.1038/s41592-022-01728-4>.
107. Fischer, D.S., Schaar, A.C., and Theis, F.J. (2023). Modeling intercellular communication in tissues using spatial graphs of cells. *Nat. Biotechnol.* 41, 332–336. <https://doi.org/10.1038/s41587-022-01467-z>.
108. Zohora, F.T., Flores-Figueroa, E., Li, J., Paliwal, D., Notta, F., and Schwartz, G.W. (2024). NEST: Spatially-Mapped Cell-Cell Communication Patterns Using a Deep Learning-Based Attention Mechanism (Cold Spring Harbor Laboratory).
109. Sang-Aram, C., Browaeys, R., Seurinck, R., and Saeys, Y. (2025). Unraveling cell-cell communication with NicheNet by inferring active ligands from transcriptomics data. *Nat. Protoc.* 20, 1439–1467. <https://doi.org/10.1038/s41596-024-01121-9>.
110. Shao, X., Li, C., Yang, H., Lu, X., Liao, J., Qian, J., Wang, K., Cheng, J., Yang, P., Chen, H., et al. (2022). Knowledge-graph-based cell-cell communication inference for spatially resolved transcriptomic data with SpaTalk. *Nat. Commun.* 13, 4429. <https://doi.org/10.1038/s41467-022-32111-8>.
111. Kim, J., Rustam, S., Mosquera, J.M., Randell, S.H., Shaykhiev, R., Rediero, A.F., and Elemento, O. (2022). Unsupervised discovery of tissue architecture in multiplexed imaging. *Nat. Methods* 19, 1653–1661. <https://doi.org/10.1038/s41592-022-01657-2>.
112. Varrone, M., Tavernari, D., Santamaría-Martínez, A., Walsh, L.A., and Cirigliello, G. (2024). CellCharter reveals spatial cell niches associated with tissue remodeling and cell plasticity. *Nat. Genet.* 56, 74–84. <https://doi.org/10.1038/s41588-023-01588-4>.
113. Qian, J.A.-O., Shao, X.A.-O., Bao, H., Fang, Y.A.-O.X., Guo, W., Li, C.A.-O., Li, A., Hua, H.A.-O., and Fan, X.A.-O. (2025). Identification and characterization of cell niches in tissue from spatial omics data at single-cell resolution. *Nat. Commun.* 16, 1693.
114. Birk, S., Bonafonte-Pardàs, I., Feriz, A.M., Boxall, A., Aguirre, E., Memi, F., Maguza, A., Yadav, A., Armingol, E., Fan, R., et al. (2025). Quantitative characterization of cell niches in spatially resolved omics data. *Nat. Genet.* 57, 897–909. <https://doi.org/10.1038/s41588-025-02120-6>.
115. Cao, J., Spielmann, M., Qiu, X., Huang, X., Ibrahim, D.M., Hill, A.J., Zhang, F., Mundlos, S., Christiansen, L., Steemers, F.J., et al. (2019). The single-cell transcriptional landscape of mammalian organogenesis. *Nature* 566, 496–502. <https://doi.org/10.1038/s41586-019-0969-x>.

116. Bergen, V., Lange, M., Peidli, S., Wolf, F.A., and Theis, F.J. (2020). Generalizing RNA velocity to transient cell states through dynamical modeling. *Nat. Biotechnol.* 38, 1408–1414. <https://doi.org/10.1038/s41587-020-0591-3>.
117. Street, K., Risso, D., Fletcher, R.B., Das, D., Ngai, J., Yosef, N., Purdom, E., and Dudoit, S. (2018). Slingshot: cell lineage and pseudotime inference for single-cell transcriptomics. *BMC Genom.* 19, 477. <https://doi.org/10.1186/s12864-018-4772-0>.
118. Lange, M., Bergen, V., Klein, M., Setty, M., Reuter, B., Bakhti, M., Lickert, H., Ansari, M., Schniering, J., Schiller, H.B., et al. (2022). CellRank for directed single-cell fate mapping. *Nat. Methods* 19, 159–170. <https://doi.org/10.1038/s41592-021-01346-6>.
119. Gulati, G.S., Sikandar, S.S., Wesche, D.J., Manjunath, A., Bharadwaj, A., Berger, M.J., Ilagan, F., Kuo, A.H., Hsieh, R.W., Cai, S., et al. (2020). Single-cell transcriptional diversity is a hallmark of developmental potential. *Science* 367, 405–411. <https://doi.org/10.1126/science.aax0249>.
120. Pham, D., Tan, X., Balderson, B., Xu, J., Grice, L.F., Yoon, S., Willis, E.F., Tran, M., Lam, P.Y., Raghubar, A., et al. (2023). Robust mapping of spatiotemporal trajectories and cell-cell interactions in healthy and diseased tissues. *Nat. Commun.* 14, 7739. <https://doi.org/10.1038/s41467-023-43120-6>.
121. Gu, Y., Liu, J., Lee, K.H., Li, C., Lu, L., Moline, J., Guan, R., and Welch, J.D. (2025). Topological velocity inference from spatial transcriptomic data. *Nat. Biotechnol.* <https://doi.org/10.1038/s41587-025-02688-8>.
122. Patel, A.P., Tirosh, I., Trombetta, J.J., Shalek, A.K., Gillespie, S.M., Wakimoto, H., Cahill, D.P., Nahed, B.V., Curry, W.T., Martuza, R.L., et al. (2014). Single-cell RNA-seq highlights intratumoral heterogeneity in primary glioblastoma. *Science* 344, 1396–1401. <https://doi.org/10.1126/science.1254257>.
123. Fan, J., Lee, H.O., Lee, S., Ryu, D.E., Lee, S., Xue, C., Kim, S.J., Kim, K., Barkas, N., Park, P.J., et al. (2018). Linking transcriptional and genetic tumor heterogeneity through allele analysis of single-cell RNA-seq data. *Genome Res.* 28, 1217–1227. <https://doi.org/10.1101/gr.228080.117>.
124. Gao, R., Bai, S., Henderson, Y.C., Lin, Y., Schalck, A., Yan, Y., Kumar, T., Hu, M., Sei, E., Davis, A., et al. (2021). Delineating copy number and clonal substructure in human tumors from single-cell transcriptomes. *Nat. Biotechnol.* 39, 599–608. <https://doi.org/10.1038/s41587-020-00795-2>.
125. Elyanow, R., Zeira, R., Land, M., and Raphael, B.J. (2021). STARCH: copy number and clone inference from spatial transcriptomics data. *Phys. Biol.* 18, 035001. <https://doi.org/10.1088/1478-3975/abbe99>.
126. Chen, L., Chang, D., Tandukar, B., Deivendran, D., Pozniak, J., Cruz-Pacheco, N., Cho, R.J., Cheng, J., Yeh, I., Marine, C., et al. (2023). STmut: a framework for visualizing somatic alterations in spatial transcriptomics data of cancer. *Genome Biol.* 24, 273. <https://doi.org/10.1186/s13059-023-03121-6>.
127. Wilson, G.W., Derouet, M., Darling, G.E., and Yeung, J.C. (2021). scSNV: accurate dscRNA-seq SNV co-expression analysis using duplicate tag collapsing. *Genome Biol.* 22, 144. <https://doi.org/10.1186/s13059-021-02364-5>.
128. Muyas, F., Sauer, C.M., Valle-Inclán, J.E., Li, R., Rahbari, R., Mitchell, T.J., Hormoz, S., and Cortés-Ciriano, I. (2024). De novo detection of somatic mutations in high-throughput single-cell profiling data sets. *Nat. Biotechnol.* 42, 758–767. <https://doi.org/10.1038/s41587-023-01863-z>.
129. Erickson, A., He, M., Berglund, E., Marklund, M., Mirzazadeh, R., Schultz, N., Kvastad, L., Andersson, A., Bergensträhle, L., Bergensträhle, J., et al. (2022). Spatially resolved clonal copy number alterations in benign and malignant tissue. *Nature* 608, 360–367. <https://doi.org/10.1038/s41586-022-05023-2>.
130. Pei, G., Min, J., Rajapakshe, K.I., Branchi, V., Liu, Y., Selvanesan, B.C., Thege, F., Sadeghian, D., Zhang, D., Cho, K.S., et al. (2025). Spatial mapping of transcriptomic plasticity in metastatic pancreatic cancer. *Nature* 642, 212–221. <https://doi.org/10.1038/s41586-025-08927-x>.
131. Yang, C., Liu, Y., Wang, X., Jia, Q., Fan, Y., Lu, Z., Shi, J., Liu, Z., Chen, G., Li, J., et al. (2025). stSNV: a comprehensive resource of SNVs in spatial transcriptome. *Nucleic Acids Res.* 53, D1224–D1234. <https://doi.org/10.1093/nar/gkae945>.
132. Kiemen, A.L., Braxton, A.M., Grahn, M.P., Han, K.S., Babu, J.M., Reichel, R., Jiang, A.C., Kim, B., Hsu, J., Armoa, F., et al. (2022). CODA: quantitative 3D reconstruction of large tissues at cellular resolution. *Nat. Methods* 19, 1490–1499. <https://doi.org/10.1038/s41592-022-01650-9>.
133. Chen, W., Zhang, P., Tran, T.N., Xiao, Y., Li, S., Shah, V.V., Cheng, H., Brannan, K.W., Youker, K., Lai, L., et al. (2025). A visual-omics foundation model to bridge histopathology with spatial transcriptomics. *Nat. Methods* 22, 1568–1582. <https://doi.org/10.1038/s41592-025-02707-1>.
134. Valanarasu, J.M.J., Xu, H., Usuyama, N., Kim, C., Wong, C., Argaw, P., Ben Shimol, R., Crabtree, A., Matlock, K., Bartlett, A.Q., et al. (2025). Multimodal AI generates virtual population for tumor microenvironment modeling. *Cell*. <https://doi.org/10.1016/j.cell.2025.11.016>.
135. Wu, E., Bieniosek, M., Wu, Z., Thakkar, N., Charville, G.W., Makky, A., Schürch, C.M., Huyghe, J.R., Peters, U., Li, C.I., et al. (2025). RÖSIE: AI generation of multiplex immunofluorescence staining from histopathology images. *Nat. Commun.* 16, 7633. <https://doi.org/10.1038/s41467-025-62346-0>.
136. Wen, H., Tang, W., Dai, X., Ding, J., Jin, W., Xie, Y., and Tang, J. (2023). CellPLM: Pre-training of Cell Language Model beyond Single Cells (Cold Spring Harbor Laboratory).
137. Wang, C., Cui, H., Zhang, A., Xie, R., Goodarzi, H., and Wang, B. (2025). scGPT-Spatial: Continual Pretraining of Single-Cell Foundation Model for Spatial Transcriptomics (Cold Spring Harbor Laboratory).
138. Schaar, A.C., Tejada-Lapuerta, A., Palla, G., Gutgesell, R., Halle, L., Minayaeva, M., Vornholz, L., Dony, L., Drummer, F., Bahrami, M., and Theis, F.J. (2024). Nichformer: A Foundation Model for Single-Cell and Spatial Omics (Cold Spring Harbor Laboratory).
139. Blampey, Q., Benkirane, H., Bercovici, N., Mulder, K., Gessain, G., Ginhoux, F., André, F., and Cournéde, P.H. (2025). Novae: a graph-based foundation model for spatial transcriptomics data. *Nat. Methods* 22, 2539–2550. <https://doi.org/10.1038/s41592-025-02899-6>.
140. Zeira, R., Land, M., Strzalkowski, A., and Raphael, B.J. (2022). Alignment and integration of spatial transcriptomics data. *Nat. Methods* 19, 567–575. <https://doi.org/10.1038/s41592-022-01459-6>.
141. (2023). STAligner enables the integration and alignment of multiple spatial transcriptomics datasets. *Nat. Comput. Sci.* 3, 831–832. <https://doi.org/10.1038/s43588-023-00543-x>.
142. Yan, X., Ang, K.S., Van Olst, L., Edwards, A., Watson, T., Zheng, R., Fan, R., Li, M., Gate, D., and Chen, J. (2024). Mosaic Integration of Spatial Multi-Omics with SpaMosaic (Cold Spring Harbor Laboratory).
143. Causier, A., Lu, T., Fitzgerald, C., Newman, A., Vu, H., Tan, X., Vo, T., Cui, C., Narayana, V.K., Whittle, J.R., et al. (2024). SpaMTP: Integrative Statistical Analysis and Visualisation of Spatial Metabolomics and Transcriptomics Data (Cold Spring Harbor Laboratory).
144. Coleman, K., Schroeder, A., Loth, M., Zhang, D., Park, J.H., Sung, J.Y., Blank, N., Cowan, A.J., Qian, X., Chen, J., et al. (2025). Resolving tissue complexity by multimodal spatial omics modeling with MISO. *Nat. Methods* 22, 530–538. <https://doi.org/10.1038/s41592-024-02574-2>.
145. Macfawn, I.P., Magnon, G., Gorecki, G., Kunning, S., Rashid, R., Kaiza, M.E., Atiya, H., Ruffin, A.T., Taylor, S., Soong, T.R., et al. (2024). The activity of tertiary lymphoid structures in high grade serous ovarian cancer is governed by site, stroma, and cellular interactions. *Cancer Cell* 42, 1864–1881.e5. <https://doi.org/10.1016/j.ccr.2024.09.007>.
146. Helmink, B.A., Reddy, S.M., Gao, J., Zhang, S., Basar, R., Thakur, R., Yizhak, K., Sade-Feldman, M., Blando, J., Han, G., et al. (2020). B cells and tertiary lymphoid structures promote immunotherapy response. *Nature* 577, 549–555. <https://doi.org/10.1038/s41586-019-1922-8>.
147. Meylan, M., Petitprez, F., Becht, E., Bouguin, A., Pupier, G., Calvez, A., Giglioli, I., Verkarre, V., Lacroix, G., Verneau, J., et al. (2022). Tertiary lymphoid structures generate and propagate anti-tumor antibody-producing plasma cells in renal cell cancer. *Immunity* 55, 527–541.e5. <https://doi.org/10.1016/j.jimmuni.2022.02.001>.
148. Xie, Y., Peng, H., Hu, Y., Jia, K., Yuan, J., Liu, D., Li, Y., Feng, X., Li, J., Zhang, X., et al. (2025). Immune microenvironment spatial landscapes of tertiary lymphoid structures in gastric cancer. *BMC Med.* 23, 59. <https://doi.org/10.1186/s12916-025-03889-3>.

149. Liu, Y., Ye, S.Y., He, S., Chi, D.M., Wang, X.Z., Wen, Y.F., Ma, D., Nie, R.C., Xiang, P., Zhou, Y., et al. (2024). Single-cell and spatial transcriptome analyses reveal tertiary lymphoid structures linked to tumour progression and immunotherapy response in nasopharyngeal carcinoma. *Nat. Commun.* 15, 7713. <https://doi.org/10.1038/s41467-024-52153-4>.
150. Fan, X., Feng, D., Wei, D., Li, A., Wei, F., Deng, S., Shen, M., Qin, C., Yu, Y., and Liang, L. (2025). Characterizing tertiary lymphoid structures associated single-cell atlas in breast cancer patients. *Cancer Cell Int.* 25, 12. <https://doi.org/10.1186/s12935-025-03635-y>.
151. Tang, Z., Bai, Y., Fang, Q., Yuan, Y., Zeng, Q., Chen, S., Xu, T., Chen, J., Tan, L., Wang, C., et al. (2025). Spatial transcriptomics reveals tryptophan metabolism restricting maturation of intratumoral tertiary lymphoid structures. *Cancer Cell* 43, 1025–1044.e14. <https://doi.org/10.1016/j.ccel.2025.03.011>.
152. Sun, L., Zhang, W., Zhao, Y., Wang, F., Liu, S., Liu, L., Zhao, L., Lu, W., Li, M., and Xu, Y. (2020). Dendritic Cells and T Cells, Partners in Atherogenesis and the Translating Road Ahead. *Front. Immunol.* 11, 1456. <https://doi.org/10.3389/fimmu.2020.01456>.
153. Nowosad, A., Marine, J.C., and Karras, P. (2023). Perivascular niches: critical hubs in cancer evolution. *Trends Cancer* 9, 897–910. <https://doi.org/10.1016/j.trecan.2023.06.010>.
154. Onubogu, U., Gatenbee, C.D., Prabhakaran, S., Wolfe, K.L., Oakes, B., Salatin, R., Vaubel, R., Szentirmai, O., Anderson, A.R., and Janiszewska, M. (2024). Spatial analysis of recurrent glioblastoma reveals perivascular niche organization. *JCI Insight* 9, e179853. <https://doi.org/10.1172/jci.insight.179853>.
155. Ren, Y., Huang, Z., Zhou, L., Xiao, P., Song, J., He, P., Xie, C., Zhou, R., Li, M., Dong, X., et al. (2023). Spatial transcriptomics reveals niche-specific enrichment and vulnerabilities of radial glial stem-like cells in malignant gliomas. *Nat. Commun.* 14, 1028. <https://doi.org/10.1038/s41467-023-36707-6>.
156. Marsh-Wakefield, F., Santhakumar, C., Ferguson, A.L., Ashhurst, T.M., Shin, J.S., Guan, F.H.X., Shields, N.J., Platt, B.J., Putri, G.H., Gupta, R., et al. (2024). Spatial mapping of the HCC landscape identifies unique intratumoral perivascular-immune neighborhoods. *Hepatol. Commun.* 8, e0540. <https://doi.org/10.1097/HCC.0000000000000540>.
157. Jansen, C.S., Prokhnevskaya, N., Master, V.A., Sanda, M.G., Carlisle, J.W., Bilen, M.A., Cardenas, M., Wilkinson, S., Lake, R., Sowalsky, A.G., et al. (2019). An intra-tumoral niche maintains and differentiates stem-like CD8 T cells. *Nature* 576, 465–470. <https://doi.org/10.1038/s41586-019-1836-5>.
158. Gill, A.L., Wang, P.H., Lee, J., Hudson, W.H., Ando, S., Araki, K., Hu, Y., Wieland, A., Im, S., Gavora, A., et al. (2023). PD-1 blockade increases the self-renewal of stem-like CD8 T cells to compensate for their accelerated differentiation into effectors. *Sci. Immunol.* 8, eadg0539. <https://doi.org/10.1126/sciimmunol.adg0539>.
159. Meiser, P., Knolle, M.A., Hirschberger, A., de Almeida, G.P., Bayerl, F., Lacher, S., Pedde, A.M., Flommersfeld, S., Hönniger, J., Stark, L., et al. (2023). A distinct stimulatory cDC1 subpopulation amplifies CD8(+) T cell responses in tumors for protective anti-cancer immunity. *Cancer Cell* 41, 1498–1515.e10. <https://doi.org/10.1016/j.ccel.2023.06.008>.
160. Di Pilato, M., Kfuri-Rubens, R., Pruessmann, J.N., Ozga, A.J., Messemaker, M., Cadilha, B.L., Sivakumar, R., Cianciaruso, C., Warner, R.D., Marangoni, F., et al. (2021). CXCR6 positions cytotoxic T cells to receive critical survival signals in the tumor microenvironment. *Cell* 184, 4512–4530.e22. <https://doi.org/10.1016/j.cell.2021.07.015>.
161. Alteber, Z., Cojocaru, G., Granit, R.Z., Barbiro, I., Wool, A., Frenkel, M., Novik, A., Shuchami, A., Liang, Y., Carmi, V.D., et al. (2024). PVRIG is Expressed on Stem-Like T Cells in Dendritic Cell-Rich Niches in Tumors and Its Blockade May Induce Immune Infiltration in Non-Inflamed Tumors. *Cancer Immunol. Res.* 12, 876–890. <https://doi.org/10.1158/2326-6066.CIR-23-0752>.
162. Gaglia, G., Burger, M.L., Ritch, C.C., Rammos, D., Dai, Y., Crossland, G.E., Tavana, S.Z., Warchol, S., Jaeger, A.M., Naranjo, S., et al. (2023). Lymphocyte networks are dynamic cellular communities in the immuno-regulatory landscape of lung adenocarcinoma. *Cancer Cell* 41, 871–886.e10. <https://doi.org/10.1016/j.ccel.2023.03.015>.
163. Oba, T., Long, M.D., Keler, T., Marsh, H.C., Minderman, H., Abrams, S.I., Liu, S., and Ito, F. (2020). Overcoming primary and acquired resistance to anti-PD-L1 therapy by induction and activation of tumor-residing cDC1s. *Nat. Commun.* 11, 5415. <https://doi.org/10.1038/s41467-020-19192-z>.
164. Zhang, Y., Wang, N., Ding, M., Yang, Y., Wang, Z., Huang, L., Zhu, W., Mellor, A.L., Hou, X., Zhou, C., et al. (2020). CD40 Accelerates the Antigen-Specific Stem-Like Memory CD8(+) T Cells Formation and Human Papilloma Virus (HPV)-Positive Tumor Eradication. *Front. Immunol.* 11, 1012. <https://doi.org/10.3389/fimmu.2020.01012>.
165. Nguema, L., Picard, F., El Hajj, M., Dupaty, L., Fenwick, C., Cardinaud, S., Wiedemann, A., Pantaleo, G., Zurawski, S., Centlivre, M., et al. (2025). Subunit protein CD40.SARS-CoV2 vaccine induces SARS-CoV-2-specific stem cell-like memory CD8(+) T cells. *EBioMedicine* 111, 105479. <https://doi.org/10.1016/j.ebiom.2024.105479>.
166. Cords, L., Tietscher, S., Anzeneder, T., Langwieder, C., Rees, M., De Souza, N., and Bodenmiller, B. (2023). Cancer-associated fibroblast classification in single-cell and spatial proteomics data. *Nat. Commun.* 14, 4294. <https://doi.org/10.1038/s41467-023-39762-1>.
167. Grout, J.A., Sirven, P., Leader, A.M., Maskey, S., Hector, E., Puisieux, I., Steffan, F., Cheng, E., Tung, N., Maurin, M., et al. (2022). Spatial Positioning and Matrix Programs of Cancer-Associated Fibroblasts Promote T-cell Exclusion in Human Lung Tumors. *Cancer Discov.* 12, 2606–2625.
168. Cords, L., Engler, S., Haberecker, M., Rüschoff, J.H., Moch, H., de Souza, N., and Bodenmiller, B. (2024). Cancer-associated fibroblast phenotypes are associated with patient outcome in non-small cell lung cancer. *Cancer Cell* 42, 396–412.e5. <https://doi.org/10.1016/j.ccel.2023.12.021>.
169. Cords, L., De Souza, N., and Bodenmiller, B. (2024). Classifying cancer-associated fibroblasts—The good, the bad, and the target. *Cancer Cell* 42, 1480–1485. <https://doi.org/10.1016/j.ccel.2024.08.011>.
170. Koppensteiner, L., Mathieson, L., O'Connor, R.A., and Akram, A.R. (2022). Cancer Associated Fibroblasts – An Impediment to Effective Anti-Cancer T Cell Immunity. *Front. Immunol.* 13, 887380.
171. Chen, Y., McAndrews, K.M., and Kalluri, R. (2021). Clinical and therapeutic relevance of cancer-associated fibroblasts. *Nat. Rev. Clin. Oncol.* 18, 792–804.
172. Elyada, E., Bolisetty, M., Laise, P., Flynn, W.F., Courtois, E.T., Burkhardt, R.A., Teinor, J.A., Belleau, P., Biffi, G., Lucito, M.S., et al. (2019). Cross-Species Single-Cell Analysis of Pancreatic Ductal Adenocarcinoma Reveals Antigen-Presenting Cancer-Associated Fibroblasts. *Cancer Discov.* 9, 1102–1123.
173. Seoane, J., and Gomis, R.R. (2017). TGF-β Family Signaling in Tumor Suppression and Cancer Progression. *Cold Spring Harb. Perspect. Biol.* 9, a022277. <https://doi.org/10.1101/cshperspect.a022277>.
174. Arora, R., Cao, C., Kumar, M., Sinha, S., Chanda, A., McNeil, R., Samuel, D., Arora, R.K., Matthews, T.W., Chandarana, S., et al. (2023). Spatial transcriptomics reveals distinct and conserved tumor core and edge architectures that predict survival and targeted therapy response. *Nat. Commun.* 14, 5029. <https://doi.org/10.1038/s41467-023-40271-4>.
175. Wu, L., Yan, J., Bai, Y., Chen, F., Xu, J., Zou, X., Huang, A., Hou, L., Zhong, Y., Jing, Z., et al. (2021). Spatially-resolved Transcriptomics Analyses of Invasive Fronts in Solid Tumors (Cold Spring Harbor Laboratory).
176. Dhatchinamoorthy, K., Colbert, J.D., and Rock, K.L. (2021). Cancer Immune Evasion Through Loss of MHC Class I Antigen Presentation. *Front. Immunol.* 12, 636568. <https://doi.org/10.3389/fimmu.2021.636568>.
177. Enfield, K.S.S., Collier, E., Lee, C., Magness, A., Moore, D.A., Sivakumar, M., Grigoriadis, K., Pich, O., Karasaki, T., Hobson, P.S., et al. (2024). Spatial Architecture of Myeloid and T Cells Orchestrates Immune Evasion and Clinical Outcome in Lung Cancer. *Cancer Discov.* 14, 1018–1047. <https://doi.org/10.1158/2159-8290.CD-23-1380>.
178. Liu, Y., Xun, Z., Ma, K., Liang, S., Li, X., Zhou, S., Sun, L., Liu, Y., Du, Y., Guo, X., et al. (2023). Identification of a tumour immune barrier in the HCC microenvironment that determines the efficacy of immunotherapy. *J. Hepatol.* 78, 770–782. <https://doi.org/10.1016/j.jhep.2023.01.011>.

179. Castiglioni, A., Yang, Y., Williams, K., Gogineni, A., Lane, R.S., Wang, A.W., Shyer, J.A., Zhang, Z., Mittman, S., Gutierrez, A., et al. (2023). Combined PD-L1/TGF β blockade allows expansion and differentiation of stem cell-like CD8 T cells in immune excluded tumors. *Nat. Commun.* 14, 4703. <https://doi.org/10.1038/s41467-023-40398-4>.
180. Greenwald, A.C., Darnell, N.G., Hoefflin, R., Simkin, D., Mount, C.W., Gonzalez Castro, L.N., Harnik, Y., Dumont, S., Hirsch, D., Nomura, M., et al. (2024). Integrative spatial analysis reveals a multi-layered organization of glioblastoma. *Cell* 187, 2485–2501.e26. <https://doi.org/10.1016/j.cell.2024.03.029>.
181. Haley, M.J., Bere, L., Minshull, J., Georgaka, S., Garcia-Martin, N., Howell, G., Coope, D.J., Roncaroli, F., King, A., Wedge, D.C., et al. (2024). Hypoxia coordinates the spatial landscape of myeloid cells within glioblastoma to affect survival. *Sci. Adv.* 10, eadj3301. <https://doi.org/10.1126/sciadv.adj3301>.
182. Baldominos, P., Barbera-Mourelle, A., Barreiro, O., Huang, Y., Wight, A., Cho, J.W., Zhao, X., Estivill, G., Adam, I., Sanchez, X., et al. (2022). Quiescent cancer cells resist T cell attack by forming an immunosuppressive niche. *Cell* 185, 1694–1708.e19. <https://doi.org/10.1016/j.cell.2022.03.033>.
183. Silvestre-Roig, C., Kalafati, L., and Chavakis, T. (2024). Neutrophils are shaped by the tumor microenvironment: novel possibilities for targeting neutrophils in cancer. *Signal Transduct. Target. Ther.* 9, 77. <https://doi.org/10.1038/s41392-024-01786-4>.
184. Amit, M., Takahashi, H., Dragomir, M.P., Lindemann, A., Gleber-Netto, F.O., Pickering, C.R., Anfossi, S., Osman, A.A., Cai, Y., Wang, R., et al. (2020). Loss of p53 drives neuron reprogramming in head and neck cancer. *Nature* 578, 449–454. <https://doi.org/10.1038/s41586-020-1996-3>.
185. Huang, Q., Hu, B., Zhang, P., Yuan, Y., Yue, S., Chen, X., Liang, J., Tang, Z., and Zhang, B. (2025). Neuroscience of cancer: unravelling the complex interplay between the nervous system, the tumor and the tumor immune microenvironment. *Mol. Cancer* 24, 24. <https://doi.org/10.1186/s12943-024-02219-0>.
186. Zahalka, A.H., and Frenette, P.S. (2020). Nerves in cancer. *Nat. Rev. Cancer* 20, 143–157. <https://doi.org/10.1038/s41568-019-0237-2>.
187. Zhong, J., Xing, X., Gao, Y., Pei, L., Lu, C., Sun, H., Lai, Y., Du, K., Xiao, F., Yang, Y., et al. (2024). Distinct roles of TREM2 in central nervous system cancers and peripheral cancers. *Cancer Cell* 42, 968–984.e9. <https://doi.org/10.1016/j.ccell.2024.05.001>.
188. Chen, M.-M., Gao, Q., Ning, H., Chen, K., Gao, Y., Yu, M., Liu, C.-Q., Zhou, W., Pan, J., Wei, L., et al. (2025). Integrated single-cell and spatial transcriptomics uncover distinct cellular subtypes involved in neural invasion in pancreatic cancer. *Cancer Cell* 43, 1656–1676.e10. <https://doi.org/10.1016/j.ccell.2025.06.020>.
189. Bullman, S. (2023). The intratumoral microbiota: From microniches to single cells. *Cell* 186, 1532–1534. <https://doi.org/10.1016/j.cell.2023.03.012>.
190. Shi, H., Shi, Q., Grodner, B., Lenz, J.S., Zipfel, W.R., Brito, I.L., and De Vlamink, I. (2020). Highly multiplexed spatial mapping of microbial communities. *Nature* 588, 676–681. <https://doi.org/10.1038/s41586-020-2983-4>.
191. Dar, D., Dar, N., Cai, L., and Newman, D.K. (2021). Spatial transcriptomics of planktonic and sessile bacterial populations at single-cell resolution. *Science* 373, eabi4882. <https://doi.org/10.1126/science.abi4882>.
192. Wong-Rolle, A., Dong, Q., Zhu, Y., Divakar, P., Hor, J.L., Kedei, N., Wong, M., Tillo, D., Conner, E.A., Rajan, A., et al. (2022). Spatial meta-transcriptomics reveal associations of intratumor bacteria burden with lung cancer cells showing a distinct oncogenic signature. *J. Immunother. Cancer* 10, e004698. <https://doi.org/10.1136/jitc-2022-004698>.
193. Galeano Niño, J.L., Ponath, F., Ajisafe, V.A., Becker, C.R., Kempchinsky, A.G., Zepeda-Rivera, M.A., Gomez, J.A., Wu, H., Terrazas, J.G., Bouzek, H., et al. (2025). Tumor-infiltrating bacteria disrupt cancer epithelial cell interactions and induce cell-cycle arrest. *Cancer Cell*. <https://doi.org/10.1016/j.ccell.2025.09.010>.
194. Zhu, Z., Cai, J., Hou, W., Xu, K., Wu, X., Song, Y., Bai, C., Mo, Y.Y., and Zhang, Z. (2023). Microbiome and spatially resolved metabolomics analysis reveal the anticancer role of gut Akkermansia muciniphila by cross-talk with intratumoral microbiota and reprogramming tumoral metabolism in mice. *Gut Microbes* 15, 2166700. <https://doi.org/10.1080/19490976.2023.2166700>.
195. Li, Y., Chang, R.B., Stone, M.L., Delman, D., Markowitz, K., Xue, Y., Coho, H., Herrera, V.M., Li, J.H., Zhang, L., et al. (2024). Multimodal immune phenotyping reveals microbial-T cell interactions that shape pancreatic cancer. *Cell Rep. Med.* 5, 101397. <https://doi.org/10.1016/j.xcrm.2024.101397>.
196. You, S., Li, S., Zeng, L., Song, J., Li, Z., Li, W., Ni, H., Xiao, X., Deng, W., Li, H., et al. (2024). Lymphatic-localized Treg-mregDC crosstalk limits antigen trafficking and restrains anti-tumor immunity. *Cancer Cell* 42, 1415–1433.e12. <https://doi.org/10.1016/j.ccel.2024.06.014>.
197. Rezzola, S., Sigmund, E.C., Halin, C., and Ronca, R. (2022). The lymphatic vasculature: An active and dynamic player in cancer progression. *Med. Res. Rev.* 42, 576–614. <https://doi.org/10.1002/med.21855>.
198. Alitalo, A., and Detmar, M. (2012). Interaction of tumor cells and lymphatic vessels in cancer progression. *Oncogene* 31, 4499–4508. <https://doi.org/10.1038/onc.2011.602>.
199. Ma, Q., Dieterich, L.C., and Detmar, M. (2018). Multiple roles of lymphatic vessels in tumor progression. *Curr. Opin. Immunol.* 53, 7–12. <https://doi.org/10.1016/j.co.2018.03.018>.
200. Zhao, L., Qiu, Z., Yang, Z., Xu, L., Pearce, T.M., Wu, Q., Yang, K., Li, F., Saulnier, O., Fei, F., et al. (2024). Lymphatic endothelial-like cells promote glioblastoma stem cell growth through cytokine-driven cholesterol metabolism. *Nat. Cancer* 5, 147–166. <https://doi.org/10.1038/s43018-023-00658-0>.
201. Salié, H., Wischer, L., D'Alessio, A., Godbole, I., Suo, Y., Otto-Mora, P., Beck, J., Neumann, O., Stenzinger, A., Schirmacher, P., et al. (2025). Spatial single-cell profiling and neighbourhood analysis reveal the determinants of immune architecture connected to checkpoint inhibitor therapy outcome in hepatocellular carcinoma. *Gut* 74, 451–466. <https://doi.org/10.1136/gutjnl-2024-332837>.
202. Sattiraju, A., Kang, S., Giotti, B., Chen, Z., Marallano, V.J., Brusco, C., Ramakrishnan, A., Shen, L., Tsankov, A.M., Hambardzumyan, D., et al. (2023). Hypoxic niches attract and sequester tumor-associated macrophages and cytotoxic T cells and reprogram them for immunosuppression. *Immunity* 56, 1825–1843.e6. <https://doi.org/10.1016/j.immuni.2023.06.017>.
203. Fan, G., Yu, B., Tang, L., Zhu, R., Chen, J., Zhu, Y., Huang, H., Zhou, L., Liu, J., Wang, W., et al. (2024). TSPAN8(+) myofibroblastic cancer-associated fibroblasts promote chemoresistance in patients with breast cancer. *Sci. Transl. Med.* 16, eadj5705. <https://doi.org/10.1126/scitranslmed.adj5705>.
204. Lee, J.Y., Reyes, N., Woo, S.H., Goel, S., Stratton, F., Kuang, C., Mansfield, A.S., LaFave, L.M., and Peng, T. (2024). Senescent fibroblasts in the tumor stroma rewire lung cancer metabolism and plasticity. Preprint at bioRxiv. <https://doi.org/10.1101/2024.07.29.605645>.
205. Fane, M.E., Chhabra, Y., Alicea, G.M., Maranto, D.A., Douglass, S.M., Webster, M.R., Rebecca, V.W., Marino, G.E., Almeida, F., Ecker, B.L., et al. (2025). Author Correction: Stromal changes in the aged lung induce an emergence from melanoma dormancy. *Nature* 638, E31. <https://doi.org/10.1038/s41586-025-08659-y>.
206. Meguro, S., Johmura, Y., Wang, T.W., Kawakami, S., Tanimoto, S., Omori, S., Okamura, Y.T., Hoshi, S., Kayama, E., Yamaguchi, K., et al. (2024). Preexisting senescent fibroblasts in the aged bladder create a tumor-permissive niche through CXCL12 secretion. *Nat. Aging* 4, 1582–1597. <https://doi.org/10.1038/s43587-024-00704-1>.
207. Peinado, H., Zhang, H., Matei, I.R., Costa-Silva, B., Hoshino, A., Rodrigues, G., Psaila, B., Kaplan, R.N., Bromberg, J.F., Kang, Y., et al. (2017). Pre-metastatic niches: organ-specific homes for metastases. *Nat. Rev. Cancer* 17, 302–317. <https://doi.org/10.1038/nrc.2017.6>.
208. Liu, Y., and Cao, X. (2016). Characteristics and Significance of the Pre-metastatic Niche. *Cancer Cell* 30, 668–681. <https://doi.org/10.1016/j.ccr.2016.09.011>.
209. Patras, L., Shaashua, L., Matei, I., and Lyden, D. (2023). Immune determinants of the pre-metastatic niche. *Cancer Cell* 41, 546–572. <https://doi.org/10.1016/j.ccr.2023.02.018>.

210. Wang, Y., Jia, J., Wang, F., Fang, Y., Yang, Y., Zhou, Q., Yuan, W., Gu, X., Hu, J., and Yang, S. (2024). Pre-metastatic niche: formation, characteristics and therapeutic implication. *Signal Transduct. Target. Ther.* 9, 236. <https://doi.org/10.1038/s41392-024-01937-7>.
211. Zhu, C., Liao, J.Y., Liu, Y.Y., Chen, Z.Y., Chang, R.Z., Chen, X.P., Zhang, B.X., and Liang, J.N. (2024). Immune dynamics shaping pre-metastatic and metastatic niches in liver metastases: from molecular mechanisms to therapeutic strategies. *Mol. Cancer* 23, 254. <https://doi.org/10.1186/s12943-024-02171-z>.
212. Halbrook, C.J., Thurston, G., Boyer, S., Anaraki, C., Jiménez, J.A., McCarthy, A., Steele, N.G., Kerk, S.A., Hong, H.S., Lin, L., et al. (2022). Differential integrated stress response and asparagine production drive symbiosis and therapy resistance of pancreatic adenocarcinoma cells. *Nat. Cancer* 3, 1386–1403. <https://doi.org/10.1038/s43018-022-00463-1>.
213. Song, Y., Na, H., Lee, S.E., Kim, Y.M., Moon, J., Nam, T.W., Ji, Y., Jin, Y., Park, J.H., Cho, S.C., et al. (2024). Dysfunctional adipocytes promote tumor progression through YAP/TAZ-dependent cancer-associated adipocyte transformation. *Nat. Commun.* 15, 4052. <https://doi.org/10.1038/s41467-024-48179-3>.
214. Rolver, M.G., Camacho-Roda, J., Dai, Y., Flinck, M., Ialchina, R., Hindkær, J., Dyrh, R.T., Bodilsen, A.N., Prasad, N.S., Baldan, J., et al. (2025). Tumor microenvironment acidosis favors pancreatic cancer stem cell properties and in vivo metastasis. *iScience* 28, 111956. <https://doi.org/10.1016/j.isci.2025.111956>.
215. Dai, Y., Knisely, A., Yano, M., Dang, M., Hinchliff, E.M., Lee, S., Welp, A., Chelvanambi, M., Lastrapes, M., Liu, H., et al. (2025). PPP2R1A mutations portend improved survival after cancer immunotherapy. *Nature* 644, 537–546. <https://doi.org/10.1038/s41586-025-09203-8>.
216. Kader, T., Lin, J.R., Hug, C.B., Coy, S., Chen, Y.A., de Brujin, I., Shih, N., Jung, E., Pelletier, R.J., Lopez Leon, M., et al. (2025). Multimodal Spatial Profiling Reveals Immune Suppression and Microenvironment Remodeling in Fallopian Tube Precursors to High-Grade Serous Ovarian Carcinoma. *Cancer Discov.* 15, 1180–1202. <https://doi.org/10.1158/2159-8290.Cd-24-1366>.
217. Huang, K.K., Ma, H., Chong, R.H.H., Uchihara, T., Lian, B.S.X., Zhu, F., Sheng, T., Srivastava, S., Tay, S.T., Sundar, R., et al. (2023). Spatiotemporal genomic profiling of intestinal metaplasia reveals clonal dynamics of gastric cancer progression. *Cancer Cell* 41, 2019–2037.e8. <https://doi.org/10.1016/j.ccr.2023.10.004>.
218. Chen, Y., Zhu, S., Liu, T., Zhang, S., Lu, J., Fan, W., Lin, L., Xiang, T., Yang, J., Zhao, X., et al. (2023). Epithelial cells activate fibroblasts to promote esophageal cancer development. *Cancer Cell* 41, 903–918.e8. <https://doi.org/10.1016/j.ccr.2023.03.001>.
219. Chang, J., Lu, J., Liu, Q., Xiang, T., Zhang, S., Yi, Y., Li, D., Liu, T., Liu, Z., Chen, X., et al. (2025). Single-cell multi-stage spatial evolutionary map of esophageal carcinogenesis. *Cancer Cell* 43, 380–397.e7. <https://doi.org/10.1016/j.ccr.2025.02.009>.
220. Risom, T., Glass, D.R., Averbukh, I., Liu, C.C., Baranski, A., Kagel, A., McCaffrey, E.F., Greenwald, N.F., Rivero-Gutiérrez, B., Strand, S.H., et al. (2022). Transition to invasive breast cancer is associated with progressive changes in the structure and composition of tumor stroma. *Cell* 185, 299–310.e18. <https://doi.org/10.1016/j.cell.2021.12.023>.
221. Zhu, B., Chen, P., Aminu, M., Li, J.R., Fujimoto, J., Tian, Y., Hong, L., Chen, H., Hu, X., Li, C., et al. (2025). Spatial and multiomics analysis of human and mouse lung adenocarcinoma precursors reveals TIM-3 as a putative target for precursor interception. *Cancer Cell* 43, 1125–1140.e10. <https://doi.org/10.1016/j.ccr.2025.04.003>.
222. Schweizer, L., Krishnan, R., Shimizu, A., Metousis, A., Kenny, H., Mendosa, R., Nordmann, T.M., Rauch, S., Kellher, L., Heide, J., et al. (2023). Spatial proteo-transcriptomic profiling reveals the molecular landscape of borderline ovarian tumors and their invasive progression. Preprint at medRxiv. <https://doi.org/10.1101/2023.11.13.23298409>.
223. Rozenblatt-Rosen, O., Regev, A., Oberdoerffer, P., Navay, T., Hupalowska, A., Rood, J.E., Ashenberg, O., Cerami, E., Coffey, R.J., Demir, E., et al. (2020). The Human Tumor Atlas Network: Charting Tumor Transitions across Space and Time at Single-Cell Resolution. *Cell* 181, 236–249. <https://doi.org/10.1016/j.cell.2020.03.053>.
224. Karimi, E., Yu, M.W., Maritan, S.M., Perus, L.J.M., Rezanejad, M., Sorin, M., Dankner, M., Fallah, P., Doré, S., Zuo, D., et al. (2023). Single-cell spatial immune landscapes of primary and metastatic brain tumours. *Nature* 614, 555–563. <https://doi.org/10.1038/s41586-022-05680-3>.
225. Khaliq, A.M., Rajamohan, M., Saeed, O., Mansouri, K., Adil, A., Zhang, C., Turk, A., Carstens, J.L., House, M., Hayat, S., et al. (2024). Spatial transcriptomic analysis of primary and metastatic pancreatic cancers highlights tumor microenvironmental heterogeneity. *Nat. Genet.* 56, 2455–2465. <https://doi.org/10.1038/s41588-024-01914-4>.
226. Wu, Y., Yang, S., Ma, J., Chen, Z., Song, G., Rao, D., Cheng, Y., Huang, S., Liu, Y., Jiang, S., et al. (2022). Spatiotemporal Immune Landscape of Colorectal Cancer Liver Metastasis at Single-Cell Level. *Cancer Discov.* 12, 134–153. <https://doi.org/10.1158/2159-8290.Cd-21-0316>.
227. Yofe, I., Shami, T., Cohen, N., Landsberger, T., Sheban, F., Stoler-Barak, L., Yalin, A., Phan, T.S., Li, B., Monteran, L., et al. (2023). Spatial and Temporal Mapping of Breast Cancer Lung Metastases Identify TREM2 Macrophages as Regulators of the Metastatic Boundary. *Cancer Discov.* 13, 2610–2631. <https://doi.org/10.1158/2159-8290.Cd-23-0299>.
228. Jazaeri, A.A., Grisham, R., Knisely, A., Spranger, S., Zamarin, D., Hillman, R.T., Lawson, B.C., Burns, K.H., Lee, S., Westin, S.N., et al. (2023). Transforming ovarian cancer care by targeting minimal residual disease. *Med* 4, 755–760. <https://doi.org/10.1016/j.medj.2023.08.004>.
229. Knisely, A., Dai, Y., Barlow, G.L., Lee, S., Lawson, B., Clark, H., Fellman, B., Yuan, Y., Lu, W., Lubo Julio, I.C., et al. (2025). Surgical and blood-based minimal residual disease in patients with ovarian cancer after frontline therapy: Clinical outcomes and translational opportunities. *Clin. Cancer Res.* 31, 4122–4135. <https://doi.org/10.1158/1078-0432.Ccr-25-0512>.
230. Keren, L., Bosse, M., Marquez, D., Angoshtari, R., Jain, S., Varma, S., Yang, S.R., Kurian, A., Van Valen, D., West, R., et al. (2018). A Structured Tumor-Immune Microenvironment in Triple Negative Breast Cancer Revealed by Multiplexed Ion Beam Imaging. *Cell* 174, 1373–1387.e19. <https://doi.org/10.1016/j.cell.2018.08.039>.
231. Jackson, H.W., Fischer, J.R., Zanotelli, V.R.T., Ali, H.R., Mechera, R., Soysal, S.D., Moch, H., Muenst, S., Varga, Z., Weber, W.P., and Bodenmiller, B. (2020). The single-cell pathology landscape of breast cancer. *Nature* 578, 615–620. <https://doi.org/10.1038/s41586-019-1876-x>.
232. Wang, X., Venet, D., Liffrange, F., Larsimont, D., Rediti, M., Stenbeck, L., Dupont, F., Rouas, G., Garcia, A.J., Craciun, L., et al. (2024). Spatial transcriptomics reveals substantial heterogeneity in triple-negative breast cancer with potential clinical implications. *Nat. Commun.* 15, 10232. <https://doi.org/10.1038/s41467-024-54145-w>.
233. Espinosa-Carrasco, G., Chiu, E., Scrivo, A., Zumbo, P., Dave, A., Betel, D., Kang, S.W., Jang, H.J., Hellmann, M.D., Burt, B.M., et al. (2024). Intra-tumoral immune triads are required for immunotherapy-mediated elimination of solid tumors. *Cancer Cell* 42, 1202–1216.e8. <https://doi.org/10.1016/j.ccr.2024.05.025>.
234. Shiao, S.L., Gouin, K.H., 3rd, Ing, N., Ho, A., Basho, R., Shah, A., Mebane, R.H., Zitser, D., Martinez, A., Mevissen, N.Y., et al. (2024). Single-cell and spatial profiling identify three response trajectories to pembrolizumab and radiation therapy in triple negative breast cancer. *Cancer Cell* 42, 70–84.e8. <https://doi.org/10.1016/j.ccr.2023.12.012>.
235. Chen, J.H., Nieman, L.T., Spurrell, M., Jorgji, V., Elmelech, L., Richieri, P., Xu, K.H., Madhu, R., Parikh, M., Zamora, I., et al. (2024). Human lung cancer harbors spatially organized stem-immunity hubs associated with response to immunotherapy. *Nat. Immunol.* 25, 644–658. <https://doi.org/10.1038/s41590-024-01792-2>.
236. Wang, X.Q., Danenberg, E., Huang, C.S., Egle, D., Callari, M., Bermejo, B., Dugo, M., Zamagni, C., Thill, M., Anton, A., et al. (2023). Spatial predictors of immunotherapy response in triple-negative breast cancer. *Nature* 621, 868–876. <https://doi.org/10.1038/s41586-023-06498-3>.
237. Schürch, C.M., Bhate, S.S., Barlow, G.L., Phillips, D.J., Noti, L., Zlobec, I., Chu, P., Black, S., Demeter, J., McIlwain, D.R., et al. (2020). Coordinated Cellular Neighborhoods Orchestrate Antitumoral Immunity at the Colorectal Cancer Invasive Front. *Cell* 182, 1341–1359.e1319. <https://doi.org/10.1016/j.cell.2020.07.005>.
238. Dhaeinaut, M., Rose, S.A., Akturk, G., Wroblewska, A., Nielsen, S.R., Park, E.S., Buckup, M., Roudko, V., Pia, L., Sweeney, R., et al. (2022). Spatial

- CRISPR genomics identifies regulators of the tumor microenvironment. *Cell* 185, 1223–1239.e20. <https://doi.org/10.1016/j.cell.2022.02.015>.
239. Binan, L., Jiang, A., Danquah, S.A., Valakh, V., Simonton, B., Bezney, J., Manguso, R.T., Yates, K.B., Nehme, R., Cleary, B., and Farhi, S.L. (2025). Simultaneous CRISPR screening and spatial transcriptomics reveal intracellular, intercellular, and functional transcriptional circuits. *Cell* 188, 2141–2158.e18. <https://doi.org/10.1016/j.cell.2025.02.012>.
240. Bülow, R.D., Hölscher, D.L., Costa, I.G., and Boor, P. (2023). Extending the landscape of omics technologies by pathomics. *NPJ Syst. Biol. Appl.* 9, 38. <https://doi.org/10.1038/s41540-023-00301-9>.
241. Jiang, W., Wang, H., Dong, X., Yu, X., Zhao, Y., Chen, D., Yan, B., Cheng, J., Zhuo, S., Wang, H., and Yan, J. (2024). Pathomics Signature for Prognosis and Chemotherapy Benefits in Stage III Colon Cancer. *JAMA Surg.* 159, 519–528. <https://doi.org/10.1001/jamasurg.2023.8015>.